

Supporting Information for

Degree of branching in poly(acrylic acid) prepared by controlled and conventional radical polymerization

Alison R. Maniego,^{a,b} Adam T. Sutton,^{a,c} Yohann Guillaneuf,^d Catherine Lefay,^d Mathias Destarac,^e
Christopher M. Fellows,^f Patrice Castignolles,^{*b} Marianne Gaborieau^{a,b}

^aWestern Sydney University (WSU), Medical Sciences Research Group (MSRG), School of Science and Health (SSH), Parramatta, Australia

^bWSU, Australian Centre for Research on Separation Science (ACROSS), SSH, Parramatta, Australia

^cUniversity of South Australia, Future Industries Institute (FII), Mawson Lakes, Australia

^dAix Marseille Univ, CNRS, Institut de Chimie Radicale UMR 7273, Marseille, France

^ePaul Sabatier University, Toulouse, France

^fUniversity of New England, Armidale, Australia

*corresponding author: p.castignolles@westernsydney.edu.au

Polymerization conditions	2
¹³ C NMR conditions	6
Quantitative NMR spectra	7
Non-quantitative NMR spectra	14
Signal assignment	17
Fraction of dead chains.....	23
Theoretical M_n values	24
M_n quantification from NMR	26
DB quantification	30
DB overestimation	33
DB quantification for poly(n-butyl acrylates) ⁴	34
Relation between branching and the relative difference between $M_{n(ex)}$ and $M_{n(th)}$	35
Presence of macromonomers.....	36
Rate coefficients of intramolecular transfer to polymer	37
References	39

Polymerization conditions

In this work, PAAs and PNaAs were synthesized using CVRP, NMP, MADIX and ATRP methods. Polymerization conditions of AA and NaAs were as specified below.

Table S1. Description of PAAs/PNaAs investigated in this work. *T* stands for temperature, *x* for conversion. XA for 2-mercaptopropionic acid methyl ester O-ethyl dithiocarbonate, MONAMS for methyl 2-[*N*-*t*-butyl-*N*-(1-diethoxyphosphoryl-2,2-dimethylpropyl)aminoxy]propionate, BB for BlocBuilder, tBA for *t*-butyl acrylate, ACVA for 4,4'-azobis(4-cyanovaleric acid), ACD for 2,2'-azobis(4-methoxy-2,4-dimethyl valeronitrile), AIBN for 2,2'-azobisisobutyronitrile, ACBN for 1,1'-azobis(cyclohexanecarbonitrile), HB for hexyl 2-bromoisobutyrate, and HDB to hexadecyl-2-bromoisobutyrate, DMF for *N,N*-dimethylformamide, and n.d. for not determined. ^a Experimental parameters were chosen aiming at a theoretical *M_n* of 10,000 for 100 % conversion.

<i>Sample code</i>	<i>Synthesis</i>	<i>Control Agent (concentration)</i>	<i>Initiator (concentration, mM)</i>	<i>Monomer (concentration, M)</i>	<i>Solvent (volume, mL)</i>	<i>Time (h)</i>	<i>T (° C)</i>	<i>x (%)</i>
NMP-AA-1	NMP	SG1 (9 mol% with respect to MONAMS)	MONAMS (0.912)	AA (3.03)	1,4-Dioxane (35)	3	120	72
NMP-AA-3	NMP	SG1 (9 mol% with respect to MONAMS)	MONAMS ^a	AA (3)	1,4-Dioxane	3	120	63
NMP-AA-4	NMP	SG1 (9 mol% with respect to BB)	BB ^a	AA (3)	1,4-Dioxane	3	120	64
NMP-AA-5	NMP	SG1 (50 mol% with respect to BB)	BB ^a	AA (3)	Water, pH = 7	1	120	31
NMP-AA-6	NMP	SG1 (15 mol% with respect to BB)	BB ^a	AA (3)	Water, pH = 7	1	90	62

NMP-tBA-1	NMP of tBA, hydrolysis	SG1 (9 mol% with respect to MONAMS)	MONAMS (0.912)	tBA (3.03)	1,4-Dioxane (35)	3	120	65
MADIX-AA-1	MADIX	AX (136 mM)	ACVA (9.2)	AA (5.6)	Water (8) / ethanol (2)	4.5	60	99
MADIX-AA-2	MADIX	AX (22 mM)	ACVA (7.1×10^{-2})	AA (2.3)	Water (8) / ethanol (2)	4.5	60	99
MADIX-AA-3	MADIX	AX (22 mM)	ACD (2.2)	AA (3.03)	1,4-Dioxane (70)	15	35	95
MADIX-AA-4	MADIX	AX (22 mM)	AIBN (2.2)	AA (3.03)	1,4-Dioxane (70)	15	60	97
MADIX-AA-5	MADIX	AX (22 mM)	ACBN (2.2)	AA (3.03)	1,4-Dioxane (70)	15	90	97
MADIX-AA-6	MADIX	AX (22 mM)	<i>t</i> -Butyl peroxide (2.2)	AA (3.03)	1,4-Dioxane (70)	15	110	91
ATRP-tBA-1	ATRP of tBA, hydrolysis		HB (133)	tBA (6.8)	Bulk	>24	90	54
ATRP-tBA-2	ATRP of tBA, hydrolysis		HDB (134)	tBA (6.8)	Bulk	25	90	38
ATRP-tBA-3	ATRP of tBA, hydrolysis		HB (289)	tBA (6.8)	Bulk	>24	90	89
CVRP-AA-1 (CONV-AA-1 in ¹)	Conventional		AIBN (26.1)	AA (3.03)	1,4-Dioxane (35)	3.5	120	n.d.

The synthesis of MADIX-AA-3 to MADIX-AA-6 was carried out in hermetic tubes equipped with a PTFE needle valve using 1,4-dioxane as solvent, AX as chain transfer agent and initiated with a series of thermal free radical initiators selected to have a half-life (5 to 38 h, see Table S7) much longer than the polymerization time. Acrylic acid (20 g, 0.278 mol, 3.03 mol L⁻¹), 1,4-dioxane (72.31 g) and AX (416.6 mg, 2 mmol, 21.86 mmol L⁻¹) were mixed together. 23.2 g of the obtained solution were placed in a tube with 0.05 mmol of the corresponding initiator, degassed with three freeze-pump-thaw cycles, sealed under vacuum and placed into a heating block with predefined temperature. After 15 h the tube was cooled, a sample was withdrawn to determine the conversion by ¹H NMR, and the polymerization mixture was precipitated twice into cold diethyl ether. The obtained residue was dried under reduced pressure to remove remaining organic solvents, dissolved in 100 mL of deionized water and freeze-dried, giving about 4 g of white solid (80 % recovery). The obtained polymers were analyzed by size-exclusion chromatography (SEC) on an Agilent 1100 HPLC system including a vacuum degasser and an isocratic pump monitored by an eclipse 2 system (Wyatt technology), a guard column Shodex SB-G and three columns Shodex OHpak in series (two SB-806 M HQ (8mm*300mm, 13μm) and one SB-802.5 HQ (8mm*300 mm, 6μm)) coupled with a refractometer (OptilabRex, Wyatt technology), a UV detector (Agilent) set at 290 nm and a multi-angle laser light scattering detector (Dawn HeleosII + QELS, 18 angles, Wyatt technology). The eluent used was an aqueous solution of NaCl (0.1 mol L⁻¹), NaH₂PO₄ (0.25 mmol L⁻¹) and Na₂HPO₄ (0.25 mmol L⁻¹). Prior to injections, samples were diluted to a concentration of 5 g L⁻¹, stirred overnight and filtered through 0.22μm Nylon filters. Values of *M_n* and *D* are reported using SEC-MALS data. The *dn/dc* value (0.1457) was measured using a PSS DnDc-2010 differential refractometer (λ=620 nm, 35 °C).

SEC analysis of samples MADIX-AA-1 and -2 with universal calibration with a viscometer was carried out with a Malvern Triple Detector Array (TDA) SEC Model 305 with an online degasser, pump and a manual injector. They were eluted through one SEC SUPREMA pre-column (particle size of 5 μm) then through three SEC SUPREMA columns (two 1000 Å, particle size of 5 μm and one 30 Å, particle size of 5 μm) from Polymer Standards Service (PSS, Mainz) with an aqueous eluent containing 0.1 mol·L⁻¹, Na₂HPO₄ and 200 ppm NaN₃ at 50 °C and 1 mL·min⁻¹ flow rate. The TDA includes the following detectors: right-angle laser light scattering (RALLS) and 7° low angle laser light scattering (LALLS) at 670 nm, refractometer and viscometer. Data was treated using OmniSEC version 4.7.0 and was plotted using OriginPro 8.5. Injections of PAA homopolymers and block copolymers used. All samples were filtered through a 0.45 μm PES or PVDF membrane filter before injection. The system was calibrated using 10 pullulan standards ranging from 342 to 708 000 g·mol⁻¹ (molar mass at the peak) with dispersity inferior to 1.27. The obtained calibration curve was fitted with a 4th order polynomial: $\log M = 142.9 - 20.76x + 1.184x^2 - 0.0301x^3 + 0.0002824x^4$ (*R*²=0.9994). Samples were injected at 8.17 g·L⁻¹ for MADIX-AA-2 and 2.01 g·L⁻¹ for MADIX-AA-1 with ethylene glycol as a flow rate marker.

SEC analysis of samples MADIX-AA-1 and -2 with MALLS detection was carried out on a system equipped with an on-line degasser, a Waters chromatography (Milford, MA) model 1515 isocratic pump, an autosampler (Waters 717), a refractometer (RI-101, Shodex)

thermostated at 25°C, a UV absorption detector (Prostar, Varian), refractive index detector (RI-101, Shodex) and a MALLS (Dawn Heleos, 18 angles, Wyatt Technology). The samples were eluted through a three-column set (8mm*300mm, 6µm particle size, 2* SB 806 M HQ columns and one SB 802.5 HQ protected by a guard column ShodexOHPak SB806-M) with an aqueous eluent containing 0.1 M NaNO₃ and 100 ppm NaN₃ at a flow rate of 1 mL·min⁻¹. All samples were filtered through 0.45 µm membrane filter before injection. Samples were injected at ~ 5 g·L⁻¹.

The SEC analysis was carried in THF after methylation for the samples synthesized by NMP and for sample CVRP-AA-1 ¹³ (with universal calibration for samples NMP-AA-1, NMP-AA-2, and CVRP-AA-1, and as PS-equivalent molar masses for samples NMP-AA-3 to 6), in THF for the PtBA precursors for samples synthesized by ATRP ⁸ (with calibration through M_n estimates from NMR), in 0.1 mol·L⁻¹ Na₂HPO₄ in water for samples MADIX-AA-1 and MADIX-AA-2 ⁶².

References here have the same numbers as in the main manuscript:

Reference 8: A. D. Wallace, A. Al-Hamzah, C. P. East, W. O. S. Doherty and C. M. Fellows, *J. Appl. Polym. Sci.*, 2010, **116**, 1165-1171.

Reference 13: A. R. Maniego, D. Ang, Y. Guillaneuf, C. Lefay, D. Gigmes, J. R. Aldrich-Wright, M. Gaborieau and P. Castignolles, *Anal. Bioanal. Chem.*, 2013, **405**, 9009-9020.

Reference 62: A. T. Sutton, E. Read, A. R. Maniego, J. J. Thevarajah, J.-D. Marty, M. Destarac, M. Gaborieau and P. Castignolles, *J. Chromatogr. A*, 2014, **1372**, 187-195

¹³C NMR conditions

Table S2. Experimental parameters for quantitative ¹³C NMR experiments. All ¹³C and ¹H NMR experiments were recorded at room temperature (25 °C).

<i>Sample</i>	<i>Solvent</i>	<i>Concentration (g·L⁻¹)</i>	<i>Number of scans (NS)</i>	<i>Repetition delay (s)</i>	<i>DEPT-135 conducted (NS)</i>
NMP-AA-1	Dioxane- <i>d</i> ₈	150	45,056	6.00	Yes (15,360)
NMP-AA-3	Dioxane- <i>d</i> ₈	150	37,328	7.00	No
NMP-AA-4	Dioxane- <i>d</i> ₈	150	49,152	8.00	Yes (14,794)
NMP-AA-5	D ₂ O / NaOD ^a	149	45,948	6.00	No
NMP-AA-6	D ₂ O / NaOD ^a	75	152,418	6.7	No
NMP-tBA-1	D ₂ O / NaOD ^a / DCl ^b	125	57,344	12.0 ^c	Yes (36,272)
NMP-tBA-1	DMSO- <i>d</i> ₆	69.9	27,653	6.00 ^c	No
MADIX-AA-1	Dioxane- <i>d</i> ₈	100	81,920	6.00	No
MADIX-AA-2	Dioxane- <i>d</i> ₈	200	81,920	6.00	Yes (1,024)
MADIX-AA-3	Dioxane- <i>d</i> ₈	200	32,768	10.0	Yes (24,155)
MADIX-AA-4	Dioxane- <i>d</i> ₈	100	81,920	10.0	Yes (45,198)
MADIX-AA-5	Dioxane- <i>d</i> ₈	200	16,774	10.0	Yes (22,770)
MADIX-AA-6	Dioxane- <i>d</i> ₈	200	14,900	10.0	Yes (24,984)
ATRP-tBA-1	Dioxane- <i>d</i> ₈	100	40,068	6.00	No
ATRP-tBA-2	Dioxane- <i>d</i> ₈	100	13,107	6.00	No
ATRP-tBA-3	D ₂ O	66.7	16,384	3.00 ^c	No
CVRP-AA-1	Dioxane- <i>d</i> ₈	100	47,512	25.0	No
Linear	D ₂ O	100	n.r. ^d	n.r. ^d	No

^a NaOD is 1 mol equivalent to acrylic acid (AA) units; ^b DCl (deuterium chloride) is ½ mol equivalent to AA units; ^c Degree of branching *DB* was not quantified and it was not checked whether the spectrum was quantitative; ^d Spectrum was not recorded

Quantitative NMR spectra

^{13}C NMR spectra were recorded for NMP-AA-4, and MADIX-AA-1-3 in this work and their *DB* quantified when possible.

DEPT-135 spectra were recorded to confirm signal assignment in some cases. In DEPT-135 spectra, CH- and CH_3 signals are positive and CH_2 signals are negative. The quaternary carbons exhibit no signal which helps confirm the assignment of the C_q branching signal.

$^1\text{H-}^1\text{H}$ COSY and $^1\text{H-}^{13}\text{C}$ HMQC spectra were also recorded for MADIX-AA-1 and -2 in order to confirm some signal assignments. Since both spectra use ^1H NMR in at least one dimension, the ^1H NMR for both these PAAs were also included.

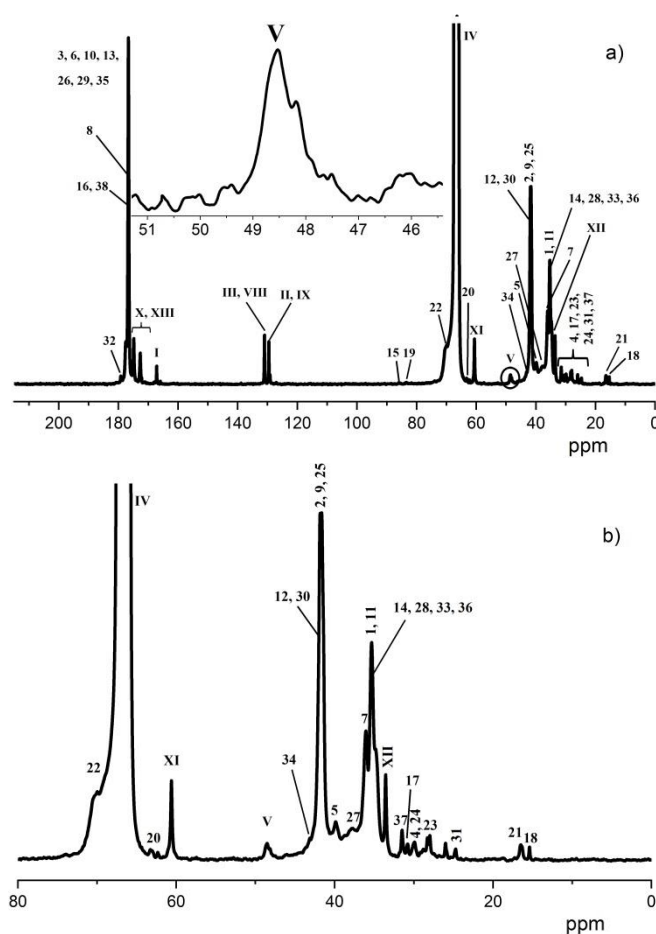


Figure S1. Solution-state quantitative ^{13}C NMR spectrum of NMP-AA-4 (75 MHz, D_2O): a) full spectrum with inset showing the region of the C_q signal of the branching point, b) 0 to 60 ppm region. See Figure S11, S12, 13b, S14a and S14c for chemical structures and Table S3 for signal assignment.

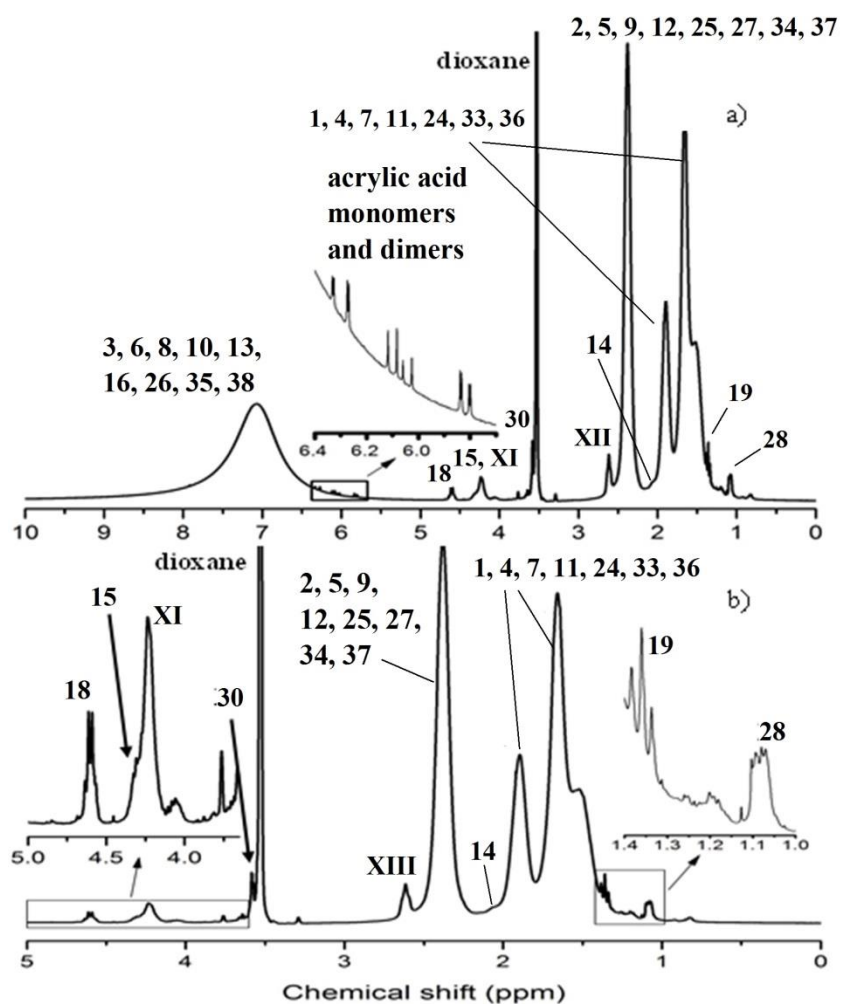


Figure S2. Solution-state ^1H NMR spectrum of MADIX-AA-1 (75.48 MHz, 1,4-dioxane- d_8): a) full spectrum with inset showing the vinylic signals from the residual monomers, b) region of the spectrum containing most signals of interest. See Figure S11, S12, S13a, S14b and S14c for chemical structures and Table S4 for signal assignment.

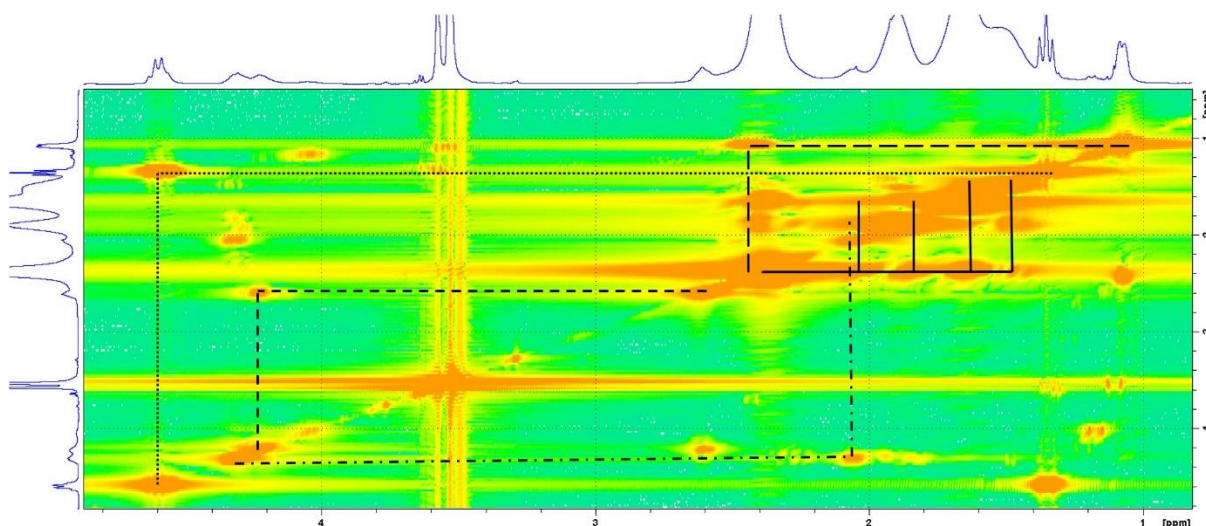


Figure S3. ^1H - ^1H COSY spectrum of MADIX-AA-1 (75.48 MHz, 1,4-dioxane- d_8). 1D spectra are shown as projections. Observed correlations were between signals 18-19 (dotted lines), XI-XII (dashed lines), 27-28 (long dashed-lines), 14-15 (dotted-dashed lines) and backbone signals (full lines). See Figure S11, S12a, S13b and S13c for the chemical structure and Table S4 for signal assignment.

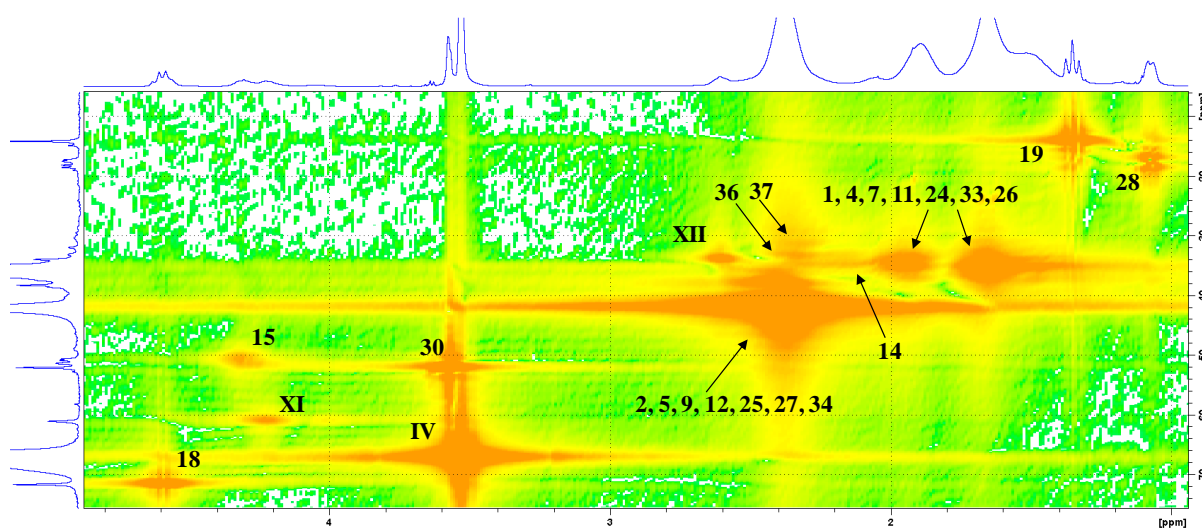


Figure S4. ^1H - ^{13}C HMQC spectrum of MADIX-AA-2 in dioxane- d_8 . Numbers represent the group assigned to cross peaks of interest (see Figure S14). 1D spectra are shown as projections. See Figure S11, S12, S13a, S14b and S14c for the chemical structure and Table S5 and S4 for signal assignment.

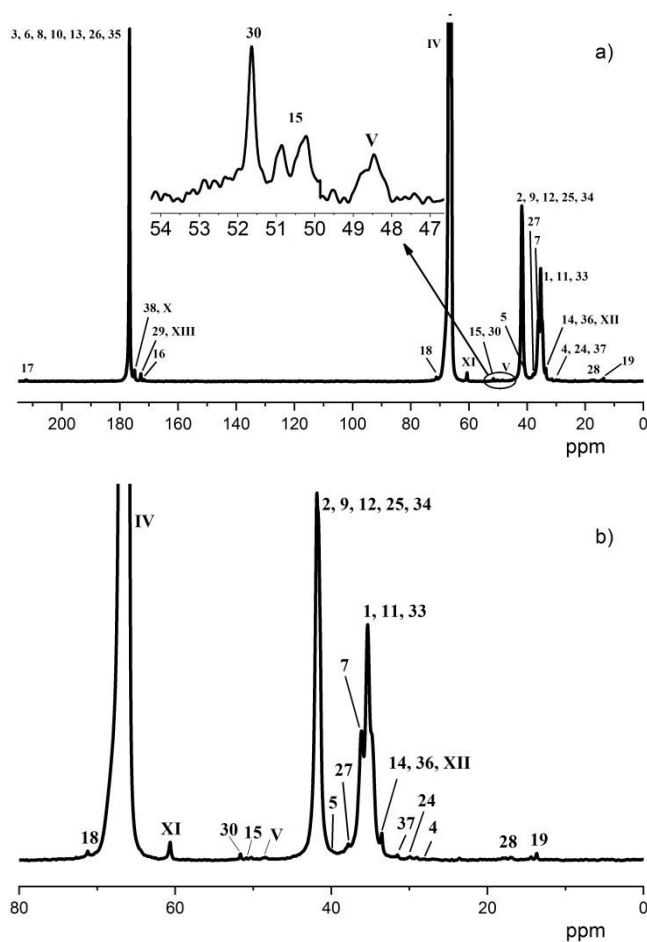


Figure S5. Solution-state quantitative ^{13}C NMR spectrum of MADIX-AA-1 (75.48 MHz, $1,4\text{-dioxane-}d_8$): a) full spectrum with inset showing the region of the C_q signal of the branching point, b) 0 to 80 ppm region. See Figure S11, S12a, S13b and S13c for chemical structures and Table S5 for the signal assignment.

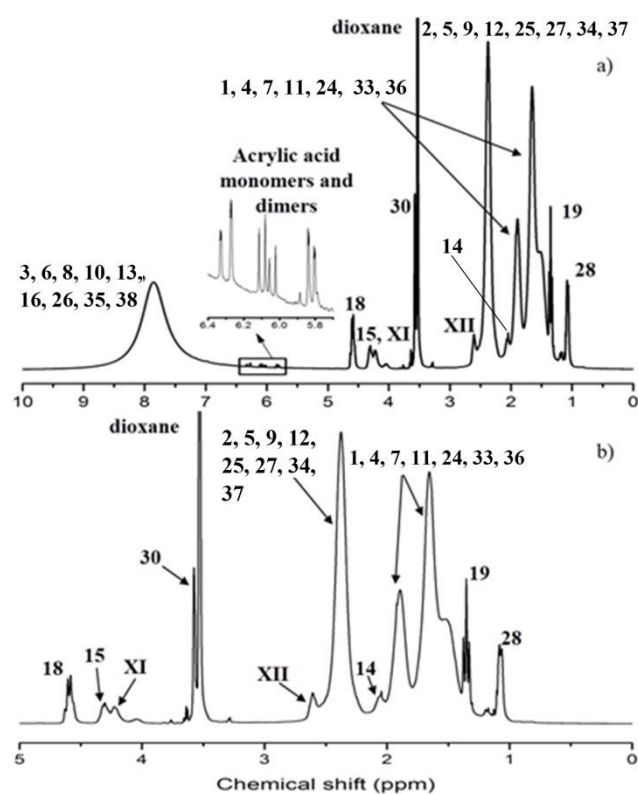


Figure S6. Solution-state ^1H NMR spectrum of MADIX-AA-2 (75.48 MHz, $1,4\text{-dioxane-}d_8$): a) full spectrum with inset showing the vinylic signals from the residual monomers/AA dimer, b) region of the spectrum containing most signals of interest. See Figure S11, S12, S13a, S14b and S14c for chemical structures and Table S4 for signal assignment.

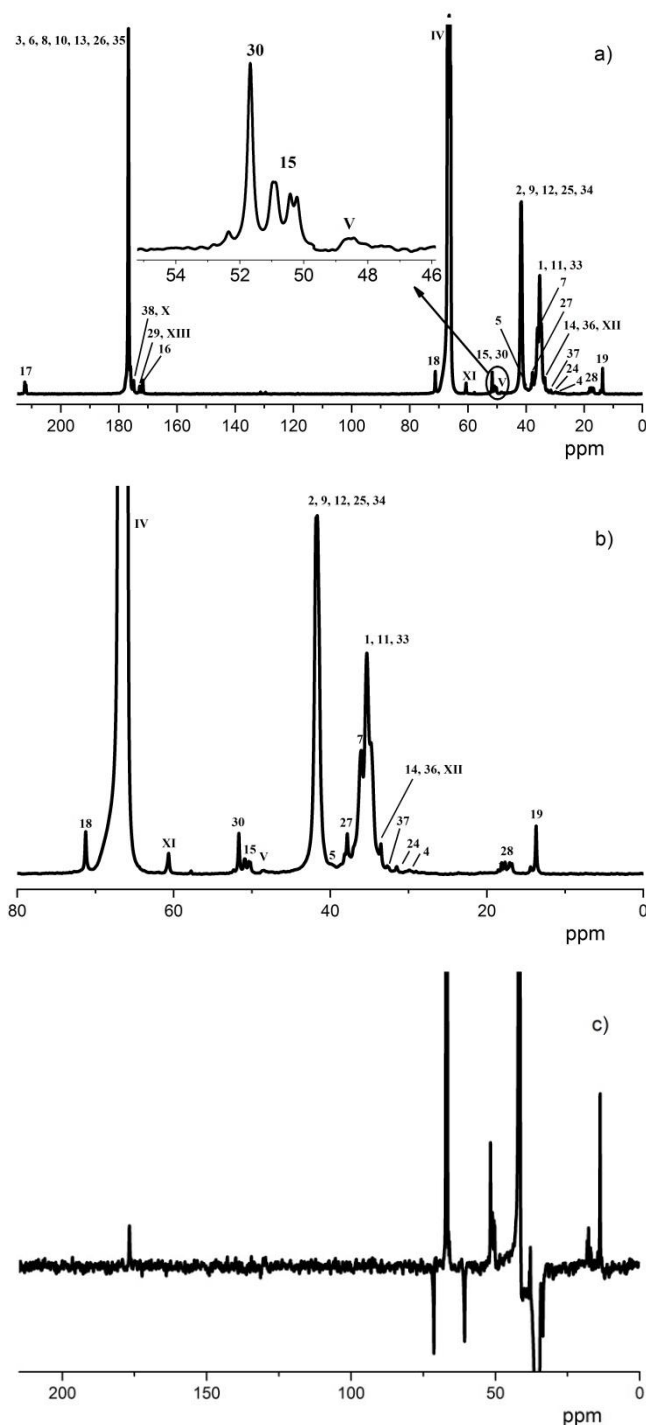


Figure S7. Solution-state ^{13}C NMR spectra of MADIX-AA-2 (75.48 MHz, 1,4-dioxane- d_8): a) full quantitative spectrum with inset showing the region of the C_q signal of the branching point, b) 0 to 80 ppm region of quantitative ^{13}C NMR spectrum and c) DEPT-135 spectrum. See Figure S11, S12, S13a, S14b and S14c for chemical structures and Table S4 for the signal assignment.

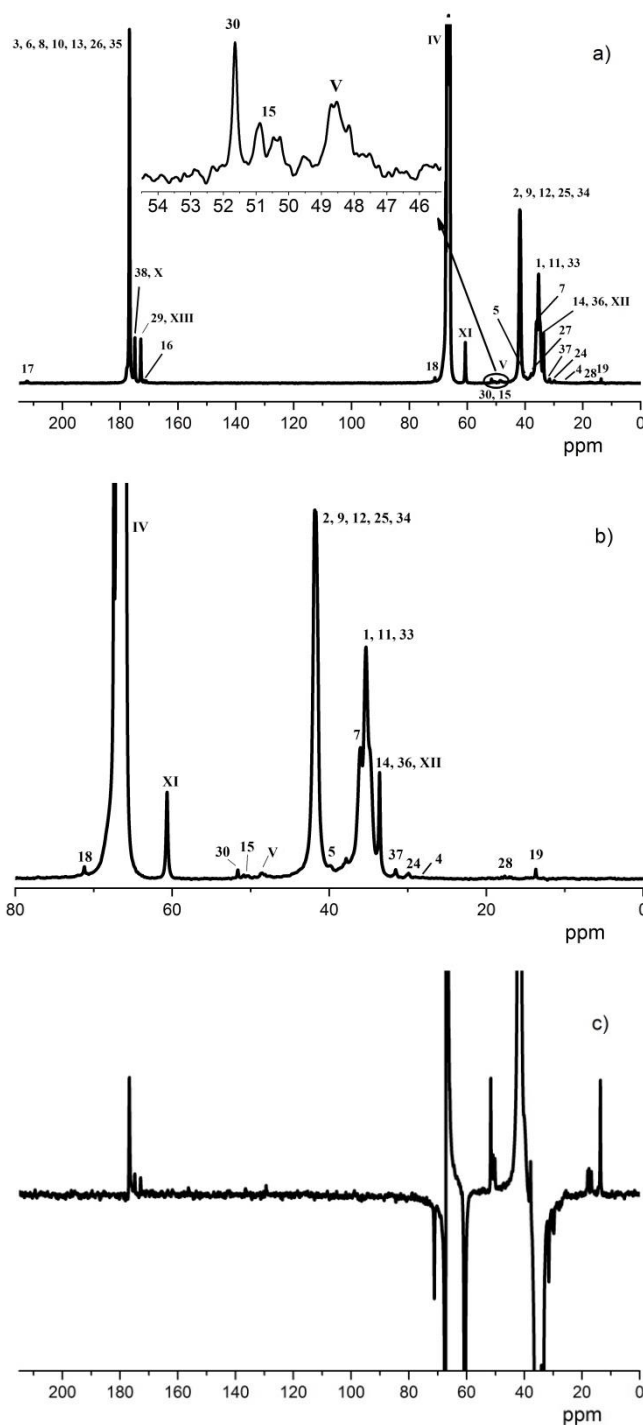


Figure S8. Solution-state ^{13}C NMR spectra of MADIX-AA-3 (75.48 MHz, $1,4\text{-dioxane-}d_8$): a) full quantitative spectrum with inset showing the region of the C_q signal of the branching point, b) 0 to 80 ppm region of quantitative ^{13}C NMR spectrum and c) DEPT-135 spectrum. See Figure S11, S12, S13a, S14b and S14c for chemical structures and Table S5 for the signal assignment.

Non-quantitative NMR spectra

Preliminary ^{13}C NMR experiments of NMP-tBA-1 and ATRP-tBA-3 showed several limitations.

Difficulties in assigning the C_q signal of NMP-tBA-1 in D_2O (Figure S9a) was encountered as the presence of sodium deuterioxide (NaOD) may have resulted in the shift of several signals. Consequently, the C_q branching may have shifted into the backbone signal and thus completely overlap with it. It is also possible that the C_q signal was below the detection limit; however, an experimental time significantly longer than the initial 4 $\frac{1}{2}$ days may be impractical. To amend the shift in the signals of NMP-tBA-1, deuterium chloride (DCl) was added (Figure S9b). No significance difference was observed between the chemical shifts of NMP-tBA-1 with and without DCl . Additionally, NMP-tBA-1 was also suspended in DMSO. No C_q signal was observed, possibly due to incomplete sample dissolution.

A high turbidity was observed for ATRP-tBA-3 in D_2O suggesting an incomplete dissolution. Incomplete solubility affects the accuracy of DB^1 , thus the C_q signal observed in the ^{13}C NMR spectrum of ATRP-tBA-3 was not representative of the branching actually present in the sample. NaOD was added to increase the sample's solubility, but it caused a shift in signals. As a result the assignment of the C_q signal could not be confirmed.

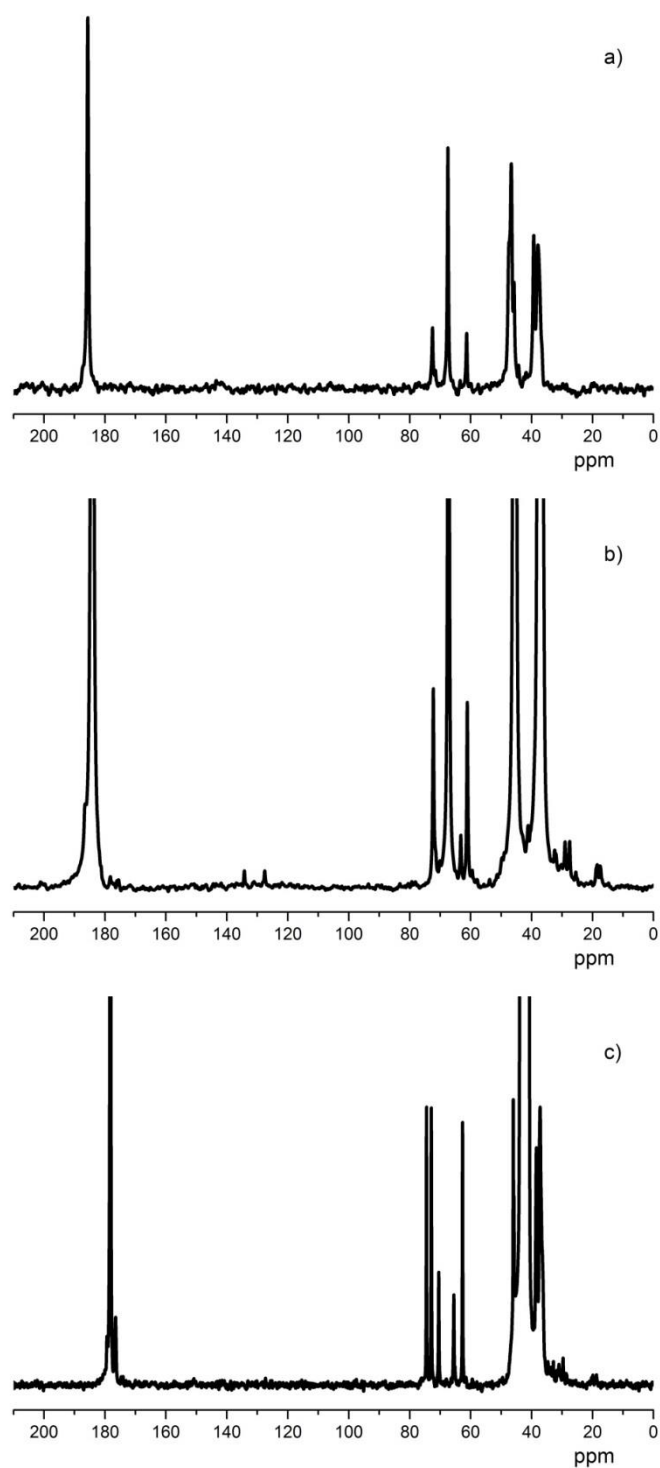


Figure S9. Solution-state ^{13}C NMR spectra of NMP-tBA-1 (75.48 MHz) in a) D_2O with NaOD, b) D_2O with NaOD and DCl and c) $\text{DMSO}-d_6$.

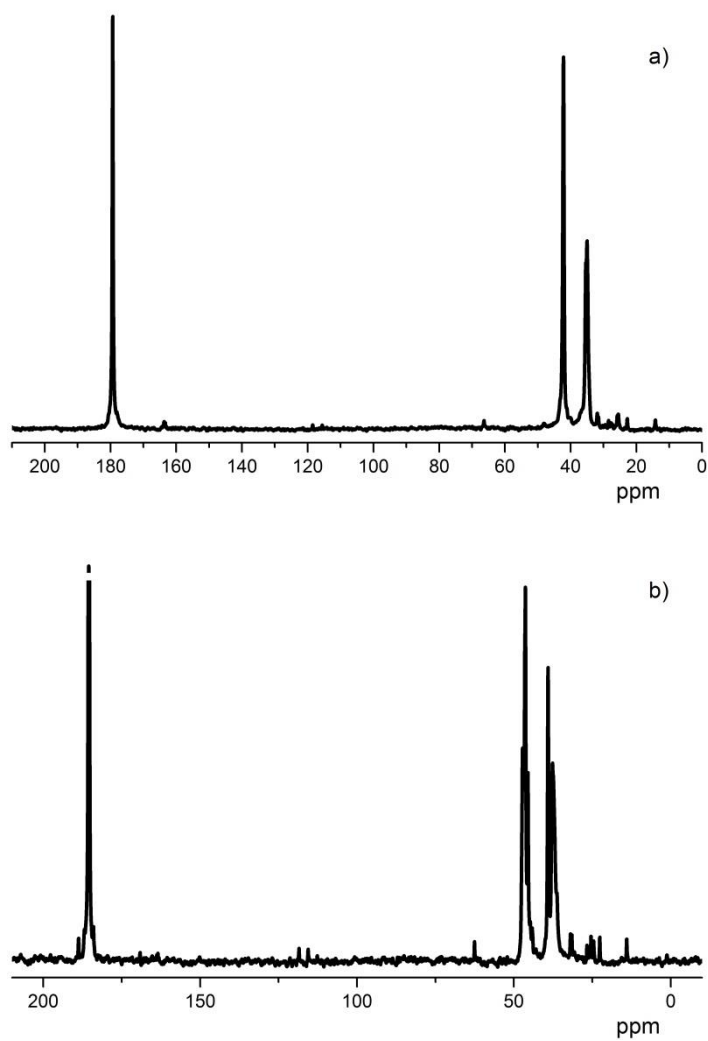


Figure S10. Solution-state ^{13}C NMR spectra of ATRP-tBA-3 (100 MHz) in a) D_2O and b) D_2O with NaOD.

Signal assignment

Full structure elucidation is shown in Table S3- S5 for the PAAs/PNaAs for which *DB* was quantified via ^{13}C NMR spectroscopy. Chemical shift estimation (Table S3-S5) was with ChemNMR (Cambridgesoft). For MADIX-AA-1 and 2, ^1H NMR and two-dimensional NMR spectra were also recorded for a comprehensive structure elucidation. For *DB* quantification the signals of interest are from C_q and the backbone. Overlapping signals of some end group with the polymer backbone ones are also accounted for in the M_n and *DB* quantification as shown in Equation S1-S26. In the case of overlapping signals, when DEPT-135 could not discriminate between the different possible assignments because the carbon atoms bear the same number of hydrogens, the signals were tentatively assigned. Presence of synthesis residues like acrylic acid and acrylic acid dimer was assumed unless confirmed otherwise via ^1H NMR spectroscopy. Chemical structures of PAA/PNaA as well as of the initiating and end groups with their group numbers have been assigned in an earlier publication (Figure S11 - S14 of ¹).

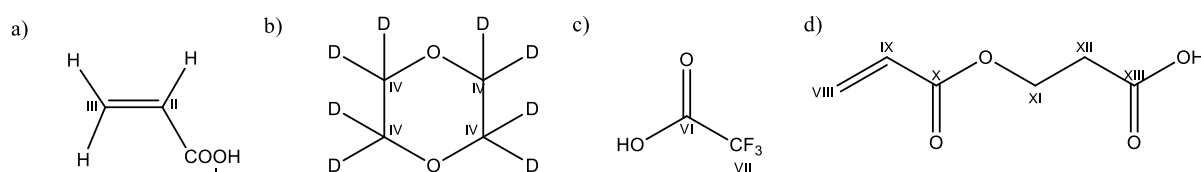


Figure S11. Chemical structure of a) AA, b) 1,4-dioxane-*d*₈, c) TFA and d) AA dimer. The labelled group numbers (GNs) are used for chemical shift assignment as published in ¹.

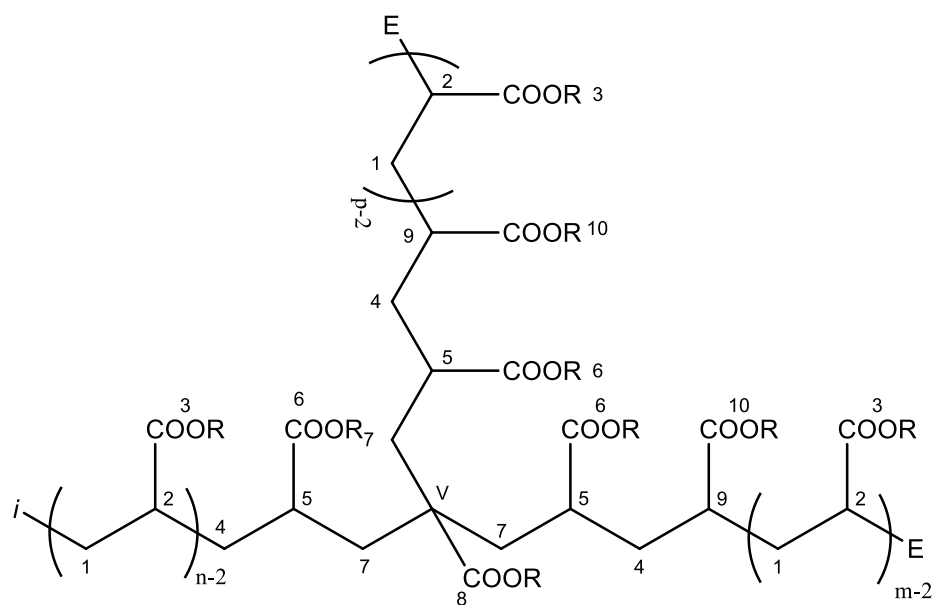


Figure S12. Chemical structure of PAAs/PNaA where R = H or R = Na. *i* represents the initiating group (see Figure S13) and *E* represents the chain-end (see Figure S14). The labelled GNs are used for chemical shift assignment as published in ¹.

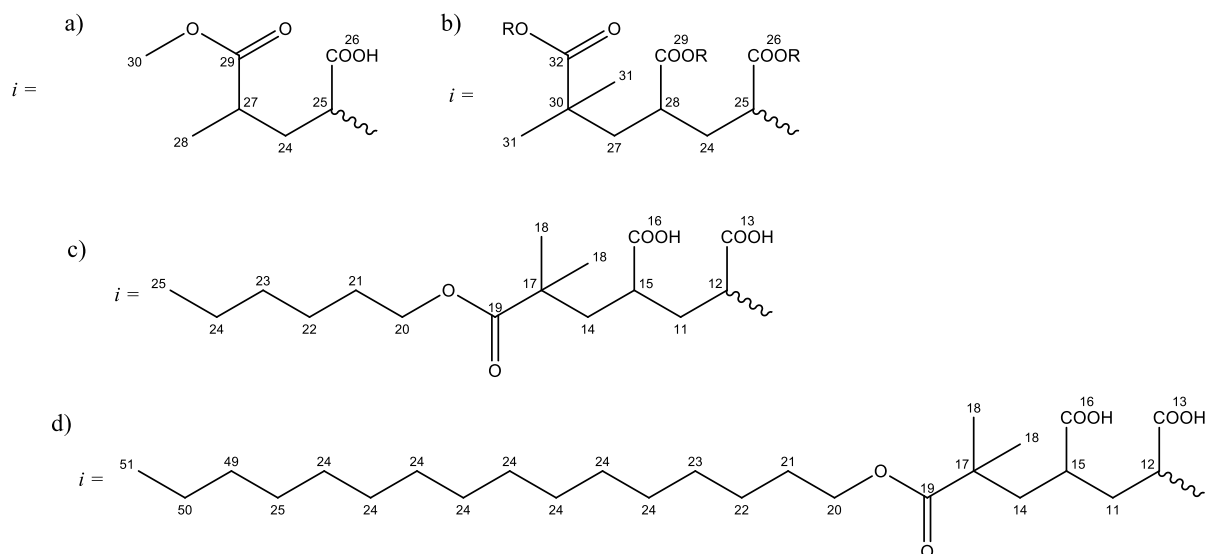


Figure S13. Chemical structure of the initiating groups (i) of a) MONAMS-initiated NMP PAA and MADIX PAA, b) BB-initiated NMP PAA/PNaA (where R = H or Na, which will be indicated accordingly in their signal assignment table), c) hexyl 2-bromoisobutyrate-initiated ATRP PAA, and d) hexadecyl-2-bromoisobutyrate-initiated ATRP PAA. The labelled GNs are used for chemical shift assignment as published in ¹.

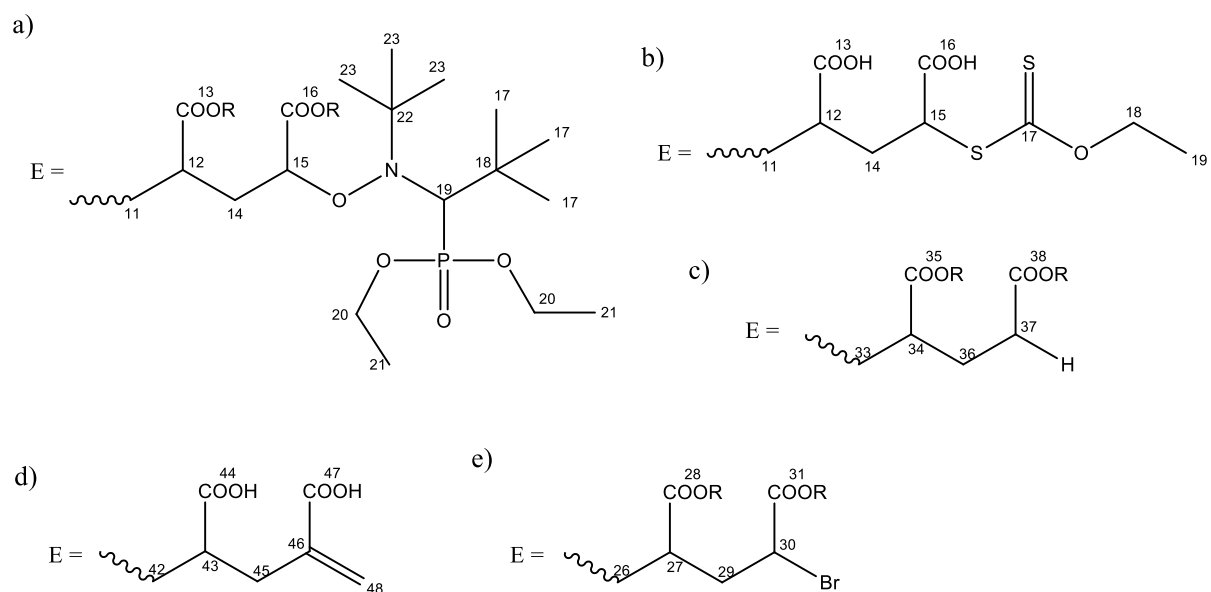


Figure S14. Chemical structure of different chain-ends (E) including the a) SG1 group, b) MADIX-agent end group, c) hydrogen, d) double-bond, e) bromine with labelled GNs that are used for chemical shift assignment as published in ¹.

Table S3. Signal assignment for ^{13}C NMR spectrum of NMP-AA-4 in dioxane- d_8 (see Figure S1 for ^{13}C NMR spectra, see Figure S11, S12, S13b, S14a and S14c for definition of GNs, where R = H). OL stands for overlapping.

<i>GN</i>	<i>Estimated δ (ppm)</i>	<i>Observed δ (ppm), NMP-AA-4</i>
1, 11	26.2	32.1 – 39.2
2, 9, 25	41.3	39.2 – 46.8
3, 6, 10, 13, 26, 29, 35	182.9	169.6 – 181.6
4, 24	26.5	30.0 (OL with 1)
5	39.1	39.9 (OL with 2)
7	45.6	36.1 (OL with 1)
8	183.7	169.6 – 181.6 (OL with 3)
12	37.3	39.2 – 46.8 (OL with 2)
14?	29.4	33.6 (OL with 1)
15	85.8	86.2 (OL with 19)
16?, 38^a?	173.2, 178.4 ^a , 177.3	169.6 – 181.6 (OL with 3)
17	26.6	30.8
18	15.3	15.4
19	81.0	83.5 (OL with 15)
20	62.2	63.3
21	16.3	16.5
22	70.4	70.0
23	26.1	28.0
27	50.0	37.8 (OL with 1)
28	38.5	32.1 – 39.2 (OL with 1)
30	41.6	39.2 – 46.8 (OL with 2)
31	24.9	24.7
32	185.1	179.5
33	25.9	32.1 – 39.2 (OL with 1)
34	43.5	43.1 (OL with 2)
36?	29.6	33.6 (OL with 1)
37	27.4	31.5 (OL with 1)
I	170.4	167.2
II, IX^a	127.5	129.5
III, VIII^a	134.1	131.0
IV	66.5	66.5
V	39.6	48.5
X, XIII	166.5, 177.3	172.0-175.6
XI	59.8	60.6
XII	33.8	33.6 (OL with 1)

^a Signals corresponding to two or more estimated δ values contain OL signals. Estimated δ values are listed in the same order as respective GNs. These signals cannot be confirmed with one-dimensional NMR only and are thus indicated by a question mark. This footnote applies to every table in this section.

Table S4. Signal assignments for ^1H NMR spectra of MADIX-AA-1 and -2 in dioxane- d_8 (see Figure S2 and S6 for ^1H NMR spectra, see Figure S11, S12, S13a, S14b and S14c for definition of GNs, where R=H).

<i>GN</i>	<i>Estimated δ (ppm)</i>	<i>Observed δ (ppm), MADIX-AA-1</i>	<i>Observed δ (ppm), MADIX-AA-2</i>
1	1.75	1.29 -2.16	1.23 – 2.16
2	2.35	2.16-2.87	2.16 – 2.87
3	11.0	5.50-8.50	6.50-9.00
4	1.75	1.29 -2.16 (OL with 1)	1.23 – 2.16 (OL with 1)
5	2.35	2.16-2.87 (OL with 2)	2.16 – 2.87 (OL with 2)
6	11.0	5.50-8.50	6.50-9.00
7	1.71	1.29 -2.16 (OL with 1)	1.23 – 2.16 (OL with 1)
8	11.0	5.50-8.50	6.50-9.00
9	2.35	2.16-2.87 (OL with 2)	2.16 – 2.87 (OL with 2)
10	11.0	5.50-8.50	6.50-9.00
11	1.75	1.29 -2.16 (OL with 1)	1.23 – 2.16 (OL with 1)
12	2.35	2.16-2.87 (OL with 2)	2.16 – 2.87 (OL with 2)
13	11.0	5.50-8.50	6.50-9.00
14	2.42	2.04-2.11 (OL with 1)	2.02-2.17 (OL with 1)
15	3.40	4.31 (OL with XI)	4.31 (OL with XI)
16	11.0	5.50-8.50	6.50-9.00
17	-	-	-
18	3.58	4.60	4.60
19	1.10	1.36 (OL with 1)	1.35 (OL with 1)
24	1.87	1.29 -2.16 (OL with 1)	1.23 – 2.16 (OL with 1)
25	2.35	2.16-2.87 (OL with 2)	2.16 – 2.87 (OL with 2)
26	11.0	5.50-8.50	6.50-9.00
27	2.49	2.16-2.87 (OL with 2)	2.16 – 2.87 (OL with 2)
28	1.19	1.08	1.08
29	-	-	-
30	3.68	3.58	3.58
33	1.75	1.29 -2.16 (OL with 1)	1.23 – 2.16 (OL with 1)
34	2.35	2.16-2.87 (OL with 2)	2.16 – 2.87 (OL with 2)
35	11.0	5.50-8.50	6.50-9.00
36	1.79	1.29 -2.16 (OL with 1)	1.23 – 2.16 (OL with 1)
37	2.33	2.16-2.87 (OL with 2)	2.16 – 2.87 (OL with 2)
38	11.0	5.50-8.50	6.50-9.00
II, III		5.80-6.34	5.80 – 6.34 ^a
XI	4.42	4.24 (OL with 15)	4.23 (OL with 15)
X11	2.51	2.55-2.68 (OL with 2)	2.59-2.66 (OL with 2)

^a The residual double bond signals were confirmed by comparing the splitting pattern observed for the residual double bond in reference ².

Table S5. Signal assignment for ^{13}C NMR spectra of MADIX-AA-1 to -3 in 1,4-dioxane- d_8 (see Figure S5, S7 and S8 respectively for ^{13}C NMR spectra, see Figure S11, S12, S13a, S14b and S14c of for definition of GNs, where R=H).

<i>GN</i>	<i>Estimated δ (ppm)</i>	<i>Observed δ (ppm), MADIX-AA-1</i>	<i>Observed δ (ppm), MADIX-AA-2</i>	<i>Observed δ (ppm), MADIX-AA-3</i>
1	26.2	27.8 – 39.2	25.9 – 39.3	24.5 – 39.2
2, 9	41.3	39.2 – 46.7	39.3 – 47.3	39.2 – 46.1
3, 6, 10, 13, 26, 35	182.9	168.3 – 182.9	169.6 – 181.2	167.6 – 182.0
4	26.5	29.0 (OL with 1)	29.0 (OL with 1)	29.0 (OL with 1)
5	39.1	39.9 (OL with 2)	40.0 (OL with 2)	39.9 (OL with 2)
7	45.6	36.1 (OL with 1)	36.1 (OL with 1)	36.1 (OL with 1)
8	183.7	168.3 – 182.9 (OL with 3)	169.6 – 181.2 (OL with 3)	167.6 – 182.0 (OL with 3)
11, 33	25.9	27.8 – 39.2 (OL with 1)	25.9 – 39.3 (OL with 1)	24.5 – 39.2 (OL with 1)
12	39.9	39.2 – 46.7 (OL with 2)	39.3 – 47.3 (OL with 2)	39.2 – 46.1 (OL with 2)
14	30.8	33.5 (OL with XII)	33.5 (OL with XII)	33.6 (OL with XII)
15	47.0	49.8 – 51.7 (OL with 30)	39.3 – 47.3 (OL with 2) 50.2 – 51.6 (OL with 30)	51.2 – 52.3 (OL with 30)
16	173.3	171.7 (OL with 3)	171.8 (OL with 3)	171.8 (OL with 3)
17	215.3	212.2	212.2	212.4
18	70.0	71.2 (OL with IV)	71.2 (OL with IV)	71.2 (OL with IV)
19	14.0	13.7	13.7	13.7
24	27.0	29.9 (OL with 1)	30.0 (OL with 1)	29.9 (OL with 1)
25	41.0	39.2 – 46.7 (OL with 2)	39.3 – 47.3 (OL with 2)	39.2 – 46.1 (OL with 2)
27	35.9	37.8 (OL with 2)	37.9 (OL with 2)	37.9 (OL with 2)
28	16.9	17.7	17.1	17.7
29	176.5	172.8 (OL with X, XIII)	172.9 (OL with X, XIII)	172.9 (OL with X, XIII)
30	52.2	51.7	51.6	51.7
34	43.5	39.2 – 46.7 (OL with 2)	39.3 – 47.3 (OL with 2)	39.2 – 46.1 (OL with 2)
36	29.6	33.5 (OL with XII)	33.5 (OL with XII)	33.6 (OL with XII)
37	27.4	31.6 (OL with 1)	31.5 (OL with 1)	31.6 (OL with 1)
38	178.4	175.0 (OL with X, XIII)	175.0 (OL with X, XIII)	174.9 (OL with X, XIII)
I	170.4	^c	^c	^c
II, IX	127.5	^c	130.0	^c
III, VIII	134.1	^c	131.6	^c
IV	66.5	66.5	66.5	66.5
V	36.0	48.5	48.5	48.5
X, XIII	166.5, 177.3	172.7 – 175.7	172.7 – 175.6	172.7 – 175.6
XI	59.8	60.7	60.6	60.6
XII	33.8	33.5	33.5	33.6

For ^a see footnote a of Table S3. ^b Signal not assigned due to no corresponding signals in the estimated δ values. ^c Monomer/AA dimer are confirmed in ^1H NMR spectroscopy but are below the LOD in ^{13}C .

Fraction of dead chains

^{13}C NMR allows to detect the hydrogen end-groups in addition to the control agent end-groups and branching points. Hydrogen end-groups are assumed to originate mainly from either transfer to polymer or termination (by combination or disproportionation). The fraction of dead chains can thus be estimated as:

$$\text{Dead chains (mol\%)} = \frac{(H - C_q) \cdot 100}{H - C_q + L} \quad (\text{S1})$$

where H is the signal integral of the $-\text{CH}_2$ end group, C_q is the signal integral of the quaternary carbon (“branching” signal, see Table S11) and L the signal integral of one carbon related to the control agent (living chain).

The results of the calculations of the dead chains are given in Table S6. Most of the ^{13}C NMR spectra exhibit a lower signal integral for the H-terminated region than for the quaternary carbon. This would numerically correspond to negative values for the fraction of dead chains. A value of 0 is simply indicated in the table in this case. The maximum possible fraction of dead chains has also been estimated based on the precision of each signal integral derived from the relevant SNR . The maximum fraction of dead chains is calculated from the highest possible value of H and the lowest value of C_q .

Table S6. Fraction of dead chains determined from ^{13}C NMR spectroscopy.

<i>Sample</i>	<i>Integration range of H signal (ppm)</i>	<i>Integration range of L signal (ppm)</i>	<i>Dead chains (mol%)</i>	<i>Maximum Dead chains (mol%)</i>
NMP-AA-1	31.13-31.25	24.84-52.57	0	0
NMP-AA-3	34.31-34.97	182.96-184.6	0	26
NMP-AA-4	31.18-31.67	25.49-23.79	0	0
NMP-AA-5 A	31.37-34.90		0	27
MADIX-AA-1	31.51-32.26	53.52-49.55	0	24
MADIX-AA-2	31.20-32.53	53.52-49.55	0.5	7
MADIX-AA-3	30.54-31.77	52.52-50.00	17	57
MADIX-AA-4 A		16.00-21.28	0	33
MADIX-AA-5 A	28.00-31.6	13.19-14.61	0	35
MADIX-AA-6	33.46-34.48	15.07-12.99	0 *	0 *
ATRP-tBA-1	30.8-32.66	12.56-15.52	0.2	13
ATRP-tBA-2	32.07-32.89	12.98-15.18	0	17

* the validity of the equation determining the fraction of dead chains is more questionable due to the possible occurrence of β -scission and polymerization of the formed macromonomers.

Theoretical M_n values

Most $M_{n(th)}$ values are from the literature (see main manuscript, Experimental, Polymerization). They are listed in Table S9.

In the case of MADIX-AA-3 to -6, a $M_{n(th)}$ of 10,000 g·mol⁻¹ was targeted for each sample using the following equation:

$$M_{n(th)} = \frac{[AA]_0}{[AX]_0} \cdot x \cdot M_{AA} + M_{AX} \quad (S2)$$

where $[AA]_0$ and $[AX]_0$ are the initial concentrations (mol·L⁻¹) in acrylic acid monomer and xanthate (AX), respectively, x is the monomer conversion, M_{AA} and M_{AX} are the molar masses of AA and AX, respectively.

$M_{n(th)}$ values have then been more accurately calculated taking the formation of dead chains into account:

$$M_{n(th)} = \frac{[AA]_0}{[AX]_0 + \frac{2f}{2-k^{ss}}[I]_0 [1-\exp(-k_d \cdot t)]} \cdot x \cdot M_{AA} + M_{AX} \quad (S3)$$

where f is the efficiency of the initiator I, k^{ss} is the fraction of termination taking place by disproportionation, $[I]_0$ is the initial initiator concentration (mol·L⁻¹), k_d is the kinetic coefficient for the decomposition of the initiator, t is the polymerization time. $[AA]_0$, $[AX]_0$, x , $[I]_0$, and t are given in Table S1. Kinetic coefficients are listed in Table S7 and discussed below.

Table S7. Kinetic coefficients used to calculate $M_{n(th)}$ for samples synthesized by MADIX in dioxane at various temperatures T_{polym} . ACD stands for 2,2'-azobis(4-methoxy-2,4-dimethyl valeronitrile), AIBN for 2,2'-azobisisobutyronitrile, ACBN for 1,1'-azobis(cyclohexanecarbonitrile),

Sample	T_{polym} (°C)	Initiator	Half-life (h) ^a	f	k^{ss}	<i>Dead chains</i> _{th} (mol%)
MADIX-AA-3	35	ACD	5	0.1 to 0.8	0 to 0.1	0.9 to 6.9
MADIX-AA-4	60	AIBN (V50)	17	0.8 ³	0 to 0.1	0.5 to 3.7
MADIX-AA-5	90	ACBN	10	0.1 to 0.8	0 to 0.1	0.6 to 5.2
MADIX-AA-6	110	tert-Butyl peroxide	38	0.1 to 0.8	0 to 0.1	0.2 to 2.0

^a from the 'Azo Polymerization Initiators Comprehensive Catalog', Wako.

In terms of initiator efficiency f , Minari et al.⁴ consider f values between 0.2 and 0.5 for acrylic acid but for potassium persulfate as initiator. Torii et al.⁵ determined efficiencies between 0.08 and 0.46 for initiation of acrylamide by non-ionic azo compounds in water. Wittenberg et al.³ applied one of these values, 0.38, for the initiation of acrylic acid polymerization by VA-086. No efficiency by thermal initiator of acrylic acid in dioxane has been published as far as we could see. We thus hypothesized that the efficiency of the thermal

initiators used for this work was between 0.1 and 0.8 (0.8 being the value for AIBN as used for acrylic acid by ³).

In terms of the fraction of termination by disproportionation in acrylic acid radical polymerization, k^{SS} , the initial literature assumed a similar contribution to termination of disproportionation and combination ($k^{SS} = 0.5$) ⁴. Minari et al.⁴ however did not observe the terminal double bonds (macromonomers) resulting from disproportionation and thus rather concluded that termination is mainly by combination (k^{SS} taken as 0). Our own NMR analysis on our samples show that macromonomers can be detected (see Figure S20) but they are detected only when the polymerization is performed at 120 °C in dioxane. This confirms that disproportionation is not the main termination mechanism and that the observed macromonomers are likely arising from some β -scission. Finally, Wittenberg et al.³ best fit their data assuming k^{SS} is 0.05. k^{SS} was thus assumed to be most likely between 0 and 0.1 for the polymerizations of MADIX-AA-3 to -6 performed at different temperatures.

The calculation of the theoretical M_n with Equation S2 includes a calculation of the theoretical fraction of dead chains with the term:

$$Dead\ chains_{th} (mol\%) = \frac{\frac{2f}{2-k^{SS}}[I]_0 [1-\exp(-k_d \cdot t)]}{[AX]_0 + \frac{2f}{2-k^{SS}}[I]_0 [1-\exp(-k_d \cdot t)]} \quad (S4)$$

The theoretical fraction of dead chains calculated from Equation S4 is listed in Table S6. The range of values is consistent with the estimates of fractions of dead chains by ¹³C NMR (Table S6).

M_n quantification from NMR

M_n was quantified using ^{13}C NMR in this work. Two ways to quantify M_n have been defined in the main manuscript (Equation 1 and 2). Like for *DB* quantification, signals overlapping with backbone signal should be taken into account. GN assignments of all the backbone signals were simplified to be GN1 for CH_2 , GN2 for CH and GN3 for $\text{C}=\text{O}$ unless specified otherwise. Particularly, GN15 was not integrated in the backbone signals as the chemical shift was too different. The equations for M_n quantification in PAAs/PNaAs for which overlapping signals with the backbone were observed are listed below, where M_m represents the molar mass of the monomer unit (which could be acrylic acid, sodium acrylate or *tert*-butyl acrylate). Table S8 indicates which equations are used for each sample.

$$M_n = \frac{I(\text{C}_q, \text{GNV} + \text{CH}_2, \text{GN1} + \text{CH}_{\text{GN2}} - \text{CH}_{\text{GN15}} + \text{CH}_3, \text{GN17, GN23} + \text{CH}_2, \text{GNXII}) - 5I(\text{CH}_3, \text{GN30}) - I(\text{CH}_2, \text{GNXI})}{2 \times I(\text{CH}_3, \text{GN30})} \times M_m \quad (\text{S5})$$

$$M_n = \frac{I(\text{C}=\text{O}_{\text{GN3}} + \text{C}=\text{O}_{\text{GN29}} + \text{C}=\text{O}_{\text{GNXIII}}) - I(\text{CH}_3, \text{GN30}) - I(\text{CH}_2, \text{GNXI})}{I(\text{CH}_3, \text{GN30})} \times M_m \quad (\text{S6})$$

$$M_n = \frac{I(\text{C}_q, \text{GNV} + \text{CH}_2, \text{GN1} + \text{CH}_{\text{GN2}} - \text{CH}_{\text{GN15}} + \text{CH}_3, \text{GN17, GN23, GN31} + \text{CH}_2, \text{GNXII} + \text{C}_q, \text{GN30}) - 8I(\text{CH}_3, \text{GN18}) - I(\text{CH}_2, \text{GNXI})}{2 \times I(\text{CH}_3, \text{GN18})} \times M_m \quad (\text{S7})$$

$$M_n = \frac{I(\text{C}=\text{O}_{\text{GN3}} + \text{C}=\text{O}_{\text{GN32}} + \text{C}=\text{O}_{\text{GNI, GNX, GNXIII}}) - I(\text{CH}_3, \text{GN18}) - I(\text{CH}_2, \text{GNXI}) - \frac{I(\text{CH}_2, \text{GNIII, GNVIII} + \text{CH}_2, \text{GNII, GNIX})}{2}}{I(\text{CH}_3, \text{GN18})} \times M_m \quad (\text{S8})$$

$$M_n = \frac{I(\text{C}_q, \text{GNV} + \text{CH}_2, \text{GN1} + \text{CH}_{\text{GN2}} - \text{CH}_{\text{GN15}} + \text{C}_{\text{GN30}} + \text{CH}_2, \text{GNXII}) - I(\text{CH}_2, \text{GNXI})}{2 \times I(\text{C}_{\text{GN18}})} \times M_m \quad (\text{S9})$$

$$M_n = \frac{I(\text{C}=\text{O}_{\text{GN3}} + \text{C}=\text{O}_{\text{GN32}} + \text{C}=\text{O}_{\text{GNXIII}}) - I(\text{C}_{\text{GN18}}) - I(\text{CH}_2, \text{GNXI})}{I(\text{C}_{\text{GN18}})} \times M_m \quad (\text{S10})$$

$$M_n = \frac{I(\text{CH}_2, \text{GN1}) + I(\text{CH}_{\text{GN2}})}{2 \times I(\text{CH}_3, \text{GN21})} \times M_m \quad (\text{S11})$$

$$M_n = \frac{I(\text{C}=\text{O}_{\text{GN3}}) - I(\text{C}_{\text{GN21}})}{I(\text{CH}_3, \text{GN21})} \times M_m \quad (\text{S12})$$

$$M_n = \frac{I(\text{C}_q, \text{GNV} + \text{CH}_2, \text{GN1} + \text{CH}_{\text{GN2}} + \text{C}_{\text{GN27}}) - I(\text{CH}_3, \text{GN19})}{2 \times I(\text{CH}_3, \text{GN19})} \times M_m \quad (\text{S13})$$

$$M_n = \frac{I(\text{C}=\text{O}_{\text{GN3}} + \text{C}=\text{O}_{\text{GN29}}) - I(\text{CH}_3, \text{GN19})}{I(\text{CH}_3, \text{GN19})} \times M_m \quad (\text{S14})$$

$$M_n = \frac{I(\text{C}_q, \text{GNV} + \text{CH}_2, \text{GN1} + \text{CH}_{\text{GN2}} + \text{C}_{\text{GN27}}) - I(\text{CH}_3, \text{GN28})}{2 \times I(\text{CH}_3, \text{GN28})} \times M_m \quad (\text{S15})$$

$$M_n = \frac{I(\text{C}=\text{O}_{\text{GN3}} + \text{C}=\text{O}_{\text{GN29}}) - I(\text{CH}_3, \text{GN28})}{I(\text{CH}_3, \text{GN28})} \times M_m \quad (\text{S16})$$

$$M_n = \frac{I(\text{C}_q, \text{GNV} + \text{CH}_2, \text{GN1} + \text{CH}_{\text{GN2}} + \text{C}_{\text{GN27}} + \text{CH}_2, \text{GNXII}) - I(\text{CH}_3, \text{GN19}) - I(\text{CH}_2, \text{GNXI})}{2 \times I(\text{CH}_3, \text{GN19})} \times M_m \quad (\text{S17})$$

$$M_n = \frac{I(\text{C}=\text{O}_{\text{GN3}} + \text{C}=\text{O}_{\text{GN29}} + \text{CH}_2, \text{GNXIII}) - I(\text{CH}_3, \text{GN19}) - I(\text{CH}_2, \text{GNXI})}{I(\text{CH}_3, \text{GN19})} \times M_m \quad (\text{S18})$$

$$M_n = \frac{I(\text{C}_q, \text{GNV} + \text{CH}_2, \text{GN1} + \text{CH}_{\text{GN2}} + \text{CH}_2, \text{GN17, GN21-24} + \text{CH}_3, \text{GN18}) - 7I(\text{CH}_3, \text{GN25})}{2 \times I(\text{CH}_3, \text{GN25})} \times M_m \quad (\text{S19})$$

$$M_n = \frac{I(C=O_{GN3}+C=O_{GN19})-I(CH_3,GN25)}{I(CH_3,GN25)} \times M_m \quad (S20)$$

$$M_n = \frac{I(C_{q,GNV}+CH_2,GN1+CH_{GN2}+CH_2,GN17-18,GN21-25,GN49-50)-17I(CH_3,GN51)}{2 \times I(CH_3,GN51)} \times M_m \quad (S21)$$

$$M_n = \frac{I(C=O_{GN3}+C=O_{GN19})-I(CH_3,GN51)}{2 \times I(CH_3,GN51)} \times M_m \quad (S22)$$

$$M_n = \frac{I(C_{q,GNV}+CH_2,GN1+CH_{GN2}+C_{GN17}+CH_3,GN18+CH_2,GNXII)-3(CN_{GN19})-I(CH_2,GNXI)}{2 \times I(CN_{GN19})} \times M_m \quad (S23)$$

$$M_n = \frac{I(C=O_{GN3}+C=O_{GNXIII})-I(CH_2,GNXI)}{I(CN_{GN19})} \times M_m \quad (S24)$$

Table S8. Equations used for M_n quantification in PAAs and PNaAs

<i>Sample</i>	<i>Equations</i>
NMP-AA-1 and -3	S5 ^a , S6
NMP-AA-4	S7 ^a , S8 ^a
NMP-AA-5	S9 ^a , S10 ^a
NMP-AA-6	S11, S12
MADIX-AA-1-3, MADIX-AA-5	S13 ^a , S14 ^{a, b}
MADIX-AA-4	S15, S16
MADIX-AA-6	S17 ^a , S18 ^a
ATRP-tBA-1	S19, S20
ATRP-tBA-2	S21, S22
CVRP-AA-1	S23, S24

^a Calculation was based on the assumption of 100 % livingness. ^b Equations S13 and S15, as well as Equations S14 and S16 can be used interchangeably for their respective samples; however, the assigned equation was preferred due to stronger signals present for that specific equation.

Table S9. $M_{n(th)}$ and $M_{n(ex)}$ of several PAAs/PNaAs. $M_{n(ex)}$ were obtained by several methods including SEC ($M_{n(SEC)}$), 1H NMR spectroscopy ($M_{n(^1H\ NMR)}$) and ^{13}C NMR spectroscopy ($M_{n(^{13}C\ NMR)}$). As mentioned, $M_{n(^{13}C\ NMR)}$ was calculated in 2 different ways as shown below. n.d. stands for not determined.

<i>Sample</i>	<i>$M_{n(th)}$ ($g \cdot mol^{-1}$)</i>	<i>$M_{n(SEC)}$ ($g \cdot mol^{-1}$)</i>	<i>$M_{n(^1H\ NMR)}$ ($g \cdot mol^{-1}$)</i>	<i>$M_{n(^{13}C\ NMR, bb)}$ ($g \cdot mol^{-1}$)</i>	<i>$M_{n(^{13}C\ NMR, COOH)}$ ($g \cdot mol^{-1}$)</i>
NMP-AA-1	4,900	6,900	n.d.	$6,810 \pm 350$	$6,810 \pm 350$
NMP-AA-3	4,600	7,800	n.d.	$6,700 \pm 400$	$6,660 \pm 400$
NMP-AA-4	4,150	7,200	n.d.	$12,270 \pm 870$	$11,730 \pm 830$
NMP-AA-5	2,100	10,000	n.d.	$5,910 \pm 470$	$5,590 \pm 440$
NMP-AA-6	2,700	12,000	n.d.	$5,980 \pm 1,400$	$6,020 \pm 1,410$
MADIX-AA-1	10,000	21,000 ^a ; 20,300 ^b	n.d.	$5,600 \pm 510$	$5,560 \pm 520$
MADIX-AA-2	2,000	2,200 ^a ; 12,400 ^b	n.d.	$1,760 \pm 50$	$1,710 \pm 50$
MADIX-AA-3	9,000 to 9,600	7,500	n.d.	$11,700 \pm 750$	$12,270 \pm 790$
MADIX-AA-4 A	9,300 to 9,600	21,900	n.d.	$2,830 \pm 110$	$2,960 \pm 120$
MADIX-AA-4 B	9,300 to 9,600	21,900	n.d.	$2,480 \pm 190$	$2,700 \pm 210$
MADIX-AA-5 A	9,100 to 9,600	20,000	n.d.	$11,180 \pm 1,360$	$11,540 \pm 1,404$
MADIX-AA-5 B	9,100 to 9,600	20,000	n.d.	$10,690 \pm 1,290$	$11,470 \pm 1,350$
MADIX-AA-6	8,900 to 9,000	17,000	n.d.	$11,660 \pm 1,390$	$11,720 \pm 1,400$
ATRP-tBA-1	6,810	2,880	4,220	$11,310 \pm 800$	$11,020 \pm 780$
ATRP-tBA-2	6,750	n.d.	9,390	$6,660 \pm 250$	$6,230 \pm 230$
CVRP-AA-1	n.d.	33,700	n.d.	$32,300 \pm 8,620$	$32,870 \pm 8,770$

^a from universal calibration; ^b from MALLS detection

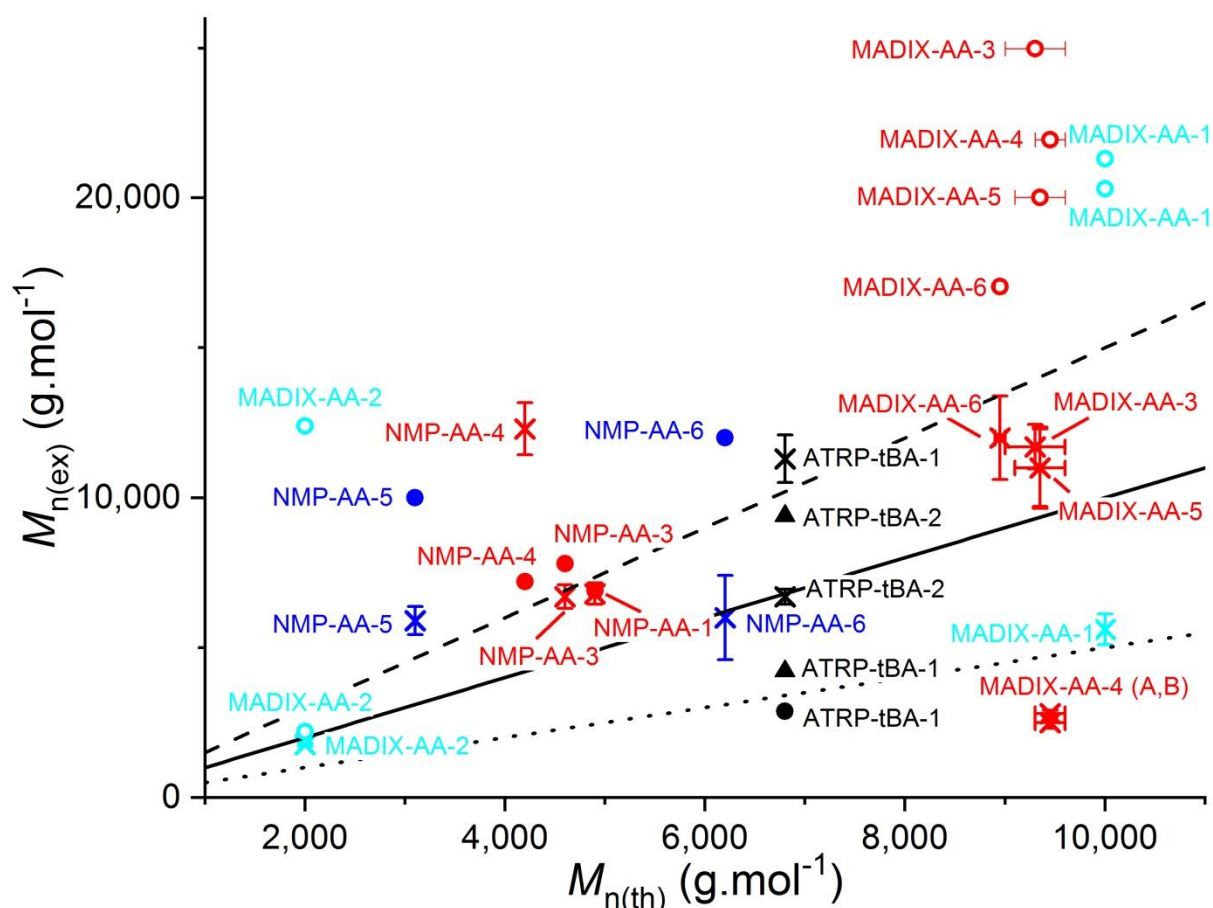


Figure S15. Larger version of Figure 1 with data points labelled with sample codes. The plotted data is also listed in Table S9. Comparison of $M_{n(th)}$ with $M_{n(ex)}$ determined for PAAs/PNaAs synthesized in dioxane using ^{13}C (×) NMR spectroscopy or organic-phase (●) and aqueous-phase (○) SEC, for PAAs/PNaAs synthesized in bulk using ^1H (▲) and ^{13}C (×) NMR spectroscopy or organic-phase SEC (●), for PAAs/PNaAs synthesized in toluene using ^1H (▲) and ^{13}C (×) NMR spectroscopy, for PAAs/PNaAs synthesized in water/ethanol using ^{13}C NMR spectroscopy (×) or aqueous-phase SEC (○), for PAAs/PNaAs synthesized in water using ^{13}C NMR spectroscopy (×) or organic-phase SEC (●). The error bars are based on the precision estimated from the sensitivity of the NMR measurement (Y error bars) or the uncertainty on some kinetic parameters (X error bars). — is the diagonal ($M_{n(th)}=M_{n(ex)}$), -- represents when $M_{n(th)}$ was 50 % lower than $M_{n(ex)}$, and represents when $M_{n(ex)}$ was 50 % lower than $M_{n(th)}$.

DB quantification

For this study, all PAA/PNaA displayed signals overlapping with the backbone signals which need to be accounted for. Two approaches allow to quantify *DB* as in ¹ (Equation 1 and 2). Similar equations were derived for *DB* quantification in PAAs/PNaAs for which signals overlap with the backbone signals (Equation S25 and S26). The slightly different chemical shifts of the signals of the backbone in the polymer were simplified to be GN1 for CH₂, GN2 for CH and GN3 for C=O for all the corresponding signals of the backbone for the equation unless specified otherwise. GNs used in these equations will refer back to the signal assignments of their corresponding sample in this supporting information and in ¹. Note that sometimes the signal for GN15 is not integrated together with the other backbone signals as it is resolved from the backbone signals.

$$DB (\%) = \frac{I(C_{q,GNV}) \times 2 \times 100}{I(C_{q,GNV}) + I(C_{q,GNV} + CH_{2,GN1} + CH_{GN2} - CH_{GN15} + CH_{3,GN17,GN23,GN31} + CH_{2,GNXII} + C_{q,GN30}) - 9I(CH_{3,GN18}) - I(CH_{2,GNXI})} \quad (S25)$$

$$DB (\%) = \frac{I(C_{q,GNV}) \times 100}{I(C=O_{GN3} + C=O_{GN32} + C=O_{GNI,GNVIII,GNX,GNXIII}) - I(CH_{3,GN18}) - 2I(CH_{2,GNXI}) - \frac{I(CH_{2,GNIII,GNVIII} + CH_{2,GNII,GNIX}) - 2I(CH_{2,GNIX})}{2}} \\ = \frac{I(C_{q,GNV}) \times 100}{I(C=O_{GN3} + C=O_{GN32} + C=O_{GNI,GNVIII,GNX,GNXIII}) - I(CH_{3,GN18}) - I(CH_{2,GNXI}) - \frac{I(CH_{2,GNIII,GNVIII} + CH_{2,GNII,GNIX})}{2}} \quad (S26)$$

Table S10. Equations used for *DB* quantification in PAAs and PNaAs

Sample	Equations
NMP-AA-1 and -3	S1 ^a of ¹ , S2 of ¹
NMP-AA-4	S25 ^a , S26 ^a
NMP-AA-5	S3 ^a of ¹ , S4 ^a of ¹
MADIX-AA-1-3 and -5	S7 ^{a,b} of ¹ , S8 ^{a,b} of ¹
MADIX-AA-4	S5 ^{a,b} of ¹ , S6 ^{a,b} of ¹
MADIX-AA-6	S9 ^a of ¹ , S10 ^a of ¹
ATRP-tBA-1	S11 of ¹ , S12 of ¹
ATRP-tBA-2	S13 of ¹ , S14 of ¹
CVRP-AA-1	S15 of ¹ , S16 of ¹

^a Calculation was based on the assumption of 100 % livingness. ^b Equations S5 and S7, as well as Equations S6 and S8 can be used interchangeably for their respective samples; however, the assigned equation was preferred due to stronger signals present for that specific equation.

Table S11. Average *DB* of several PAAs/PNaAs quantified through the signals from the backbone (Equation 1 or one of its derivatives) or the carboxylic acid group (Equation 2 or one of its derivatives). NMP-AA-6 displayed a C_q signal below detection limit and thus its *DB* was not quantified.

<i>Sample</i>	<i>Integration range of C_q signal (ppm)</i>	<i>DB (%) backbone</i>	<i>DB (%) COOH</i>
NMP-AA-1	46.7 - 50.0	3.1 ± 0.2	3.1 ± 0.2
NMP-AA-3	46.5 - 50.9	3.3 ± 0.2	3.4 ± 0.2
NMP-AA-4	46.7 - 50.8	3.2 ± 0.2	3.4 ± 0.2
NMP-AA-5 A	49.5 – 53.2	2.0 ± 0.6	2.1 ± 0.7
NMP-AA-6		$< 1.2^b$	
MADIX-AA-1	47.6 - 49.5	0.3 ± 0.1	0.3 ± 0.1
MADIX-AA-2	46.5 - 49.5	0.7 ± 0.1	0.7 ± 0.1
MADIX-AA-3	46.1 – 49.9	1.2 ± 0.2	1.2 ± 0.2
MADIX-AA-4 A	46.5 – 49.6	2.4 ± 0.2	2.3 ± 0.1
MADIX-AA-4 B	46.7 – 49.9	2.1 ± 0.1	1.9 ± 0.1
MADIX-AA-5 A	47.0 – 49.5	2.3 ± 0.2	2.3 ± 0.2
MADIX-AA-5 B	47.0 – 49.5	2.5 ± 0.3	2.4 ± 0.2
MADIX-AA-6	47.0 – 49.7	3.3 ± 0.2	3.3 ± 0.2
ATRP-tBA-1 ^a	46.5 - 50.1	1.6 ± 0.3	1.7 ± 0.3
ATRP-tBA-2 ^a	46.4 - 49.3	1.1 ± 0.1	1.1 ± 0.2
CVRP-AA-1	46.3 - 50.0	2.6 ± 0.2	2.6 ± 0.2

^a *DB* is an overestimated value because of a possible overlap between GNV and GN17 (GN17 not taken into account in the *DB* quantification). ^b The C_q signal had an SNR < 3, *DB* was overestimated via 1-point calibration (see next section).

DB overestimation

For NMP-AA-6 the C_q signal was below the detection limit (signal-to-noise ratio $SNR < 3$). It also overlapped with the backbone. Hence, the DB value was overestimated through the determination of the maximal possible DB value, DB_{\max} . A one point calibration between the ratio of the $SNRs$ of the backbone and C_q signals (SNR_{BB}/SNR_{Cq}) and the ratio of the integrals of the backbone and C_q signals (I_{BB}/I_{Cq}) was established using sample NMP-AA-3. This 1-point calibration was then used to estimate the maximal possible value of I_{Cq}/I_{BB} based on a maximal possible SNR_{Cq} value of 3 and on the experimental value of SNR_{BB} for NMP-AA-6. This was in turn used to determine DB_{\max} as follows:

$$DB_{\max} (\%) = \frac{\left(\frac{I_{Cq}}{I_{BB}}\right)_{\max} \times 200}{1 + \left(\frac{I_{Cq}}{I_{BB}}\right)_{\max}} \quad (S27)$$

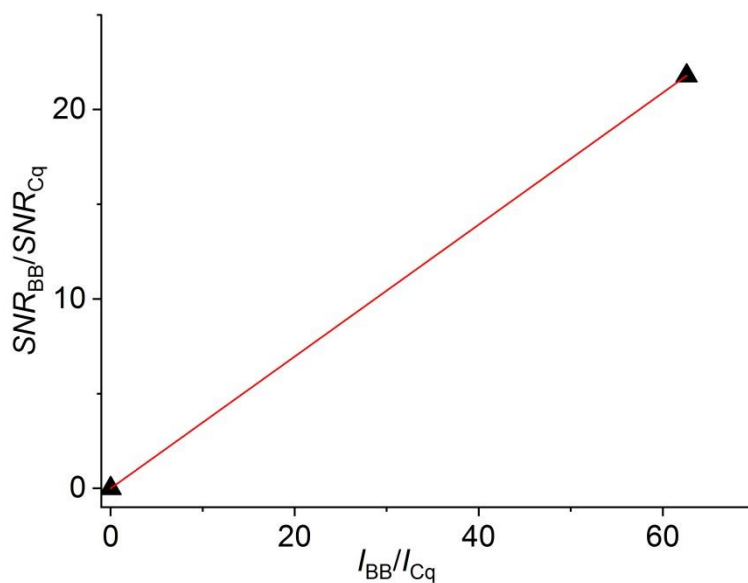


Figure S17. 1-point calibration of SNR_{BB}/SNR_{Cq} vs I_{BB}/I_{Cq} established with NMP-AA-3 . $y = 0.34829 x$

DB quantification for poly(*n*-butyl acrylates)⁶

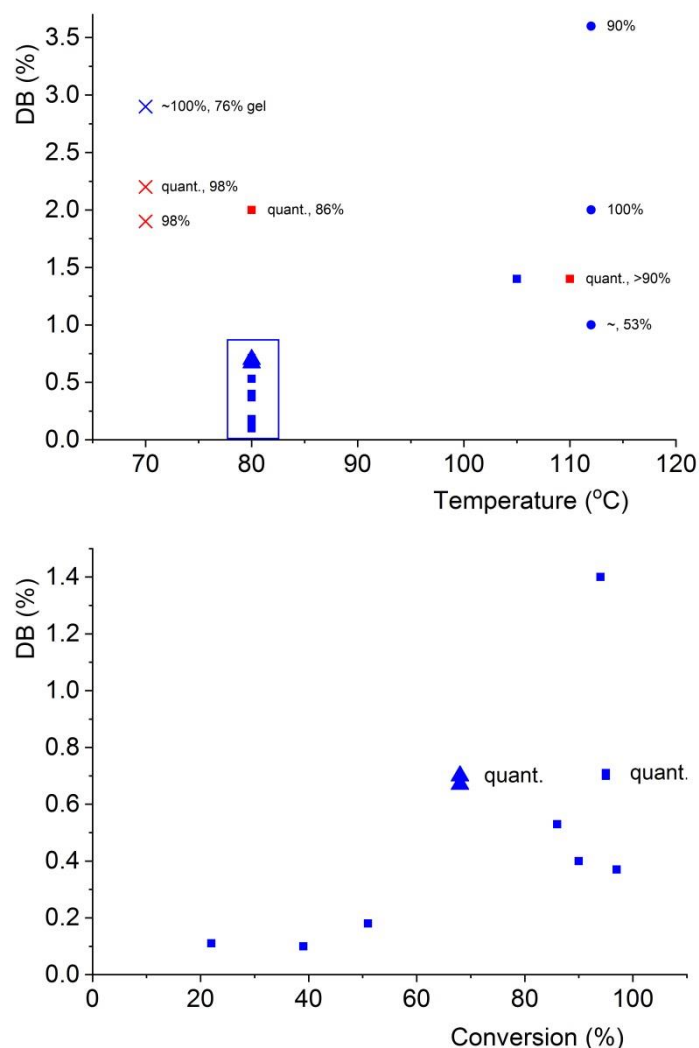


Figure S18. DB(%) of several poly(*n*-butyl acrylate)s reported in ⁶. They were synthesized at different temperatures and with different polymerization techniques including CVRP (cross), ATRP (square), RAFT (triangle) and NMP (circle) either in bulk (blue) or in 50 % xylene (red). On the top graph DB is plotted versus temperature. The percentages shown next to the data points are conversion values. The label ‘76% gel’ identifies a sample reported in ⁶ as containing 76% gel fraction. The region boxed in the top graph represents poly(*n*-butyl acrylate)s with similar DB(%) synthesized at the same temperature; the data from this region was also plotted as DB(%) versus conversion (bottom graph). DB values obtained from quantitative NMR spectra are identified through the label ‘quant.’ next to the corresponding data point. No error bar is shown since the uncertainty was not given in reference ⁶.

Relation between branching and the relative difference between $M_{n(ex)}$ and $M_{n(th)}$

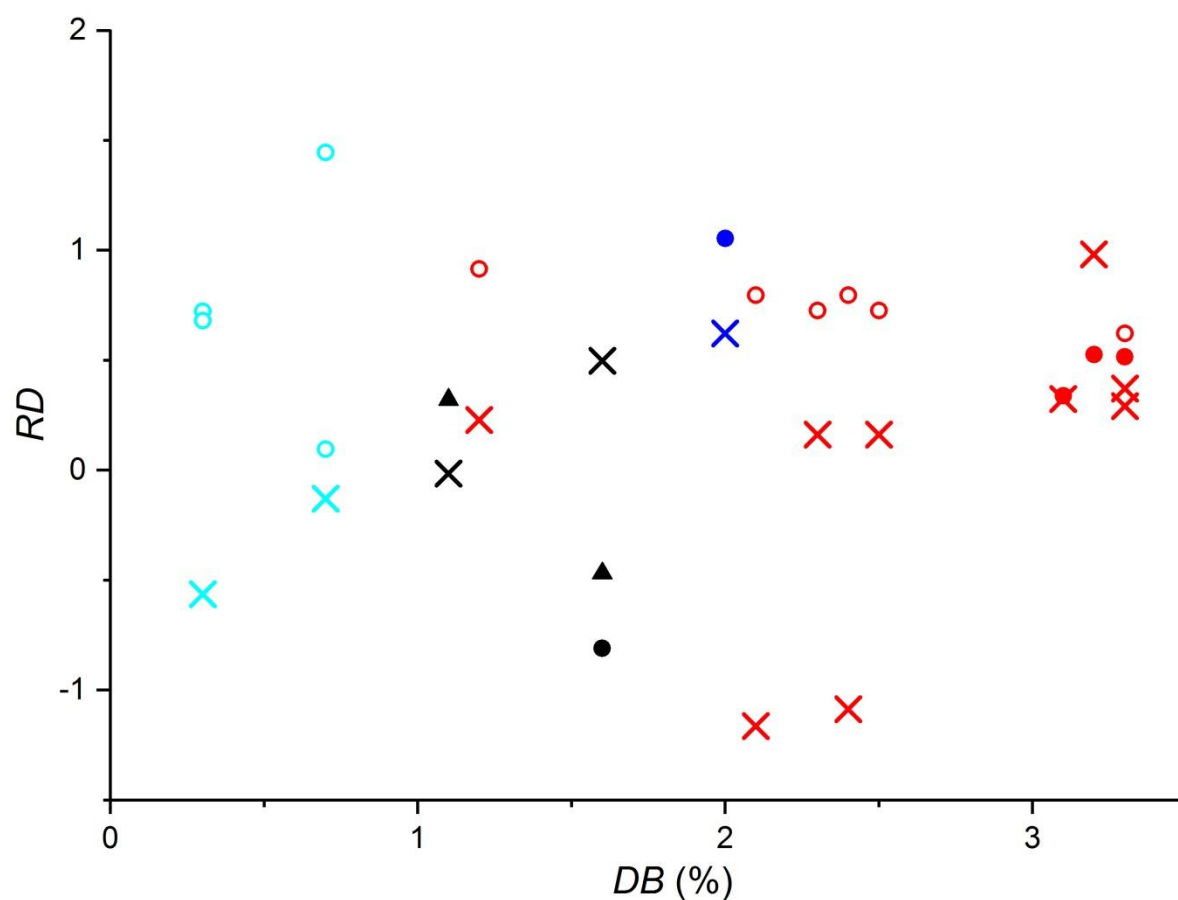


Figure S19. Relative difference (RD) between $M_{n(ex)}$ and $M_{n(th)}$ plotted as a function of DB (%) for PAAs/PNaAs synthesized in dioxane using ^{13}C (×) NMR spectroscopy or organic-phase (●) and aqueous-phase (○) SEC, for PAAs/PNaAs synthesized in bulk using ^1H (▲) and ^{13}C (×) NMR spectroscopy or organic-phase SEC (●), for PAAs/PNaAs synthesized in water/ethanol using ^{13}C NMR spectroscopy (×) or aqueous-phase SEC (○), for PAAs/PNaAs synthesized in water using ^{13}C NMR spectroscopy (×) or aqueous-phase SEC (○).

Presence of macromonomers

The presence of macromonomers due to β -scission was observed for several PAAs synthesized via NMP at 120 °C (NMP-AA-1, NMP-AA-3 and NMP-AA-4). These signals overlapped with the residual monomer signals (as shown in ²) which were also observed in all the mentioned samples.

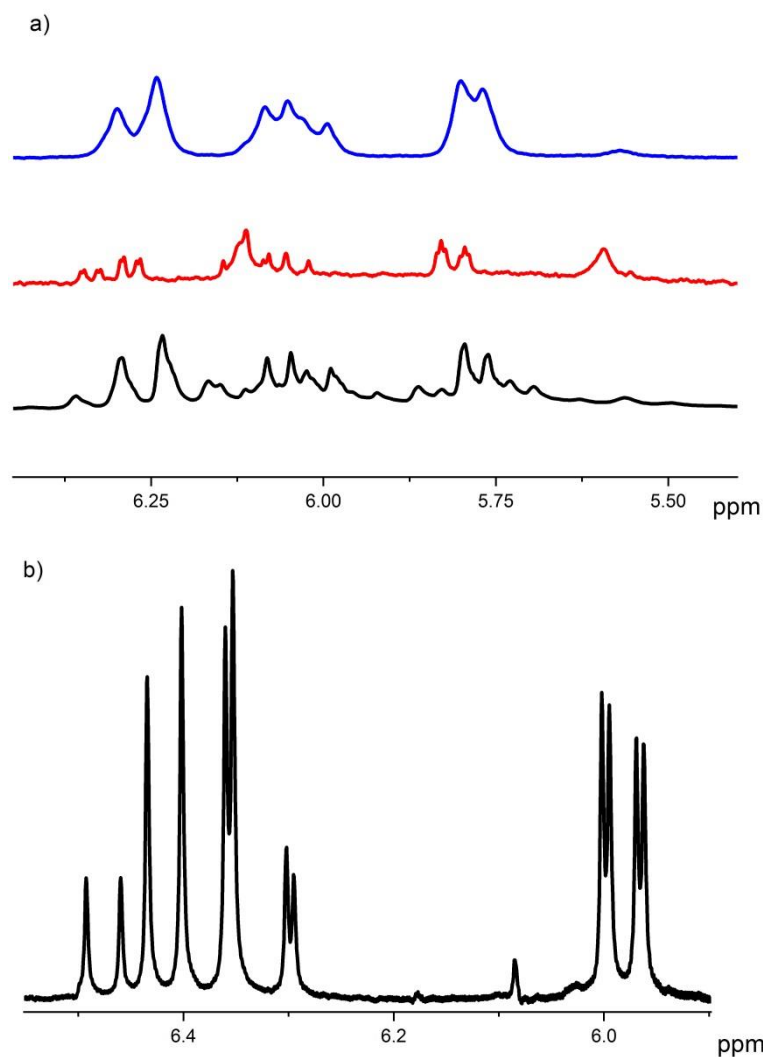


Figure S20. ¹H NMR spectra of a) NMP-AA-1 (black), NMP-AA-3 (red) and NMP-AA-4 (blue) confirming the presence of macromonomers. b) Reference spectrum of the residual monomer².

Rate coefficients of intramolecular transfer to polymer

Ratios of the rate coefficient of intramolecular transfer to polymer to the rate coefficient of propagation, k_{bb}/k_p , were estimated using the following equation:⁷

$$DB = \frac{k_{bb} 100 \cdot \ln([M]_0 / [M]_e)}{k_p ([M]_0 - [M]_e)} \quad (S28)$$

which can be rearranged into:

$$\frac{k_{bb}}{k_p} = \frac{DB \cdot ([M]_0 - [M]_e)}{100 \cdot \ln([M]_0 / [M]_e)} \quad (S29)$$

and where DB is the degree of branching, $[M]_0$ is the initial monomer concentration, and $[M]_e$ is the final monomer concentration. The assumptions must be made that every transfer to polymer event leads to branching and that the incidence of the following events may be disregarded: intermolecular chain transfer to polymer, MCR patching, β -scission and termination by disproportionation, as well as monomer consumption via addition to MCR.

k_{bb}/k_p ratios were quantified for samples MADIX-AA-3 to -6, NMP-AA-1, -3, and -4, as well as CVRP-AA-1, using $[M]_0$ given in Table S1, $[M]_e$ determined from $[M]_0$ and conversion from Table S1, and DB given in Table S11. The determined k_{bb}/k_p values are listed in Table S12 and plotted on Figure 3.

Table S12. Ratios of the rate coefficient of intramolecular transfer to polymer to the rate coefficient of propagation, k_{bb}/k_p , for several polymerizations of AA/NaA (see Table S1 for more experimental polymerization parameters). $1000/T$ is the inverse polymerization temperature.

<i>Experiment code</i>	<i>1000/T (K⁻¹)</i>	<i>k_{bb}/k_p</i>
NMP-AA-1	2.54	0.848 ± 0.065
NMP-AA-3	2.54	1.110 ± 0.067
NMP-AA-4	2.54	1.080 ± 0.068
NMP-AA-5A	2.54	0.050 ± 0.016
NMP-AA-5 B	2.54	0.031 ± 0.013
NMP-AA-6	2.75	0.012 ± 0.012
MADIX-AA-1	3.00	0.00243 ± 0.00081
MADIX-AA-2	3.00	0.00276 ± 0.00039
MADIX-AA-3	3.25	0.0115 ± 0.0019
MADIX-AA-4 A	3.00	0.02012 ± 0.00084
MADIX-AA-4 B	3.00	0.01760 ± 0.00084
MADIX-AA-5 A	2.75	0.0193 ± 0.0017
MADIX-AA-5 B	2.75	0.0210 ± 0.0017
MADIX-AA-6	2.61	0.0378 ± 0.0017
CVRP-AA-1 *	2.83	0.0706 ± 0.0054, 0.0308 ± 0.0023

* two values were calculated for this samples for conversions of 0.2 and 0.9.

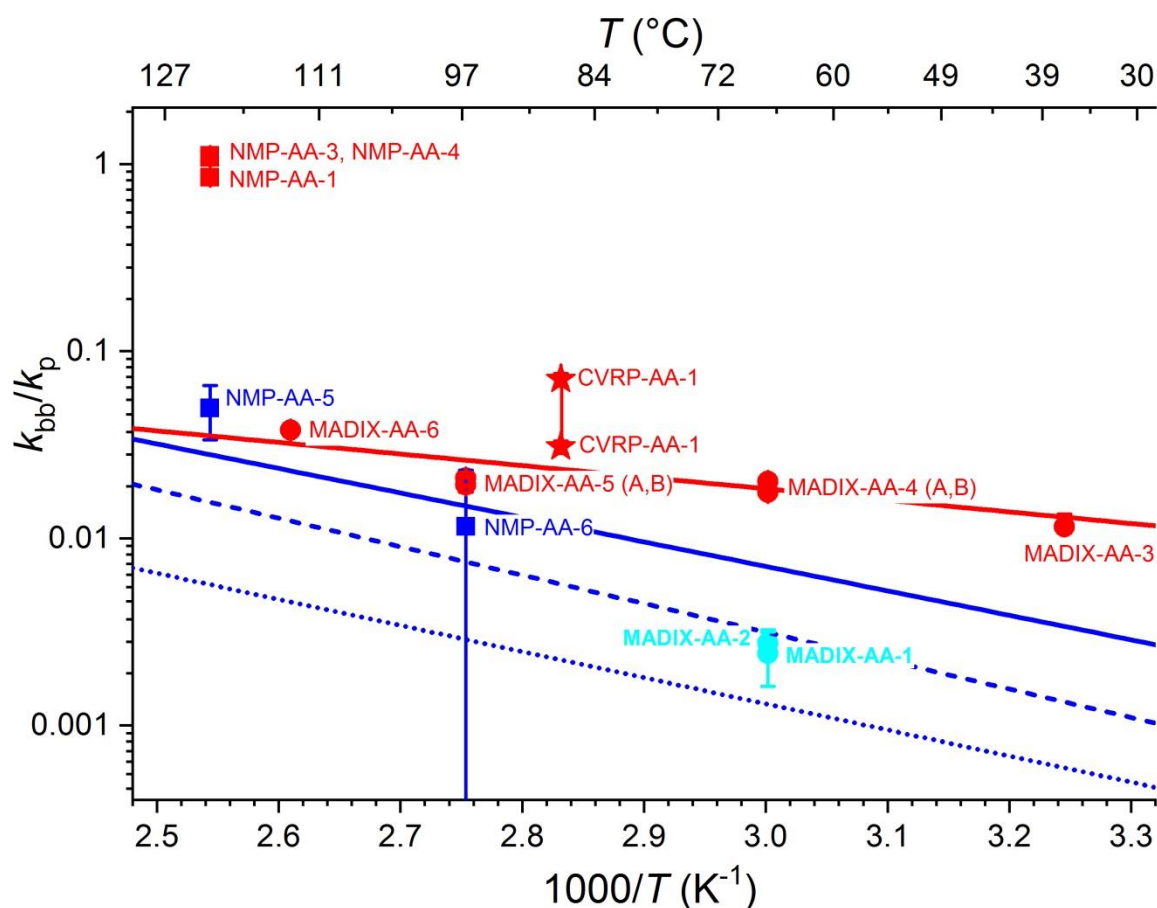


Figure S21. Larger version of Figure 3 with data points labelled with sample codes. The plotted data is also listed in Table S12. Arrhenius plot of k_{bb}/k_p for AA/NaA in dioxane by NMP (■), MADIX (●) and CVRP (★), in toluene with CVRP with CTA (☆), in water with NMP (■), in water/ethanol with MADIX (●). The error bars are based on the precision estimated from the sensitivity of the NMR measurement. — represents the Arrhenius fit for MADIX in 1,4-dioxane- d_8 ($\ln y = -1425x + 0.28$). -- and represent Arrhenius fits from previous studies with CVRP in water: with and without CTA⁸ ($\ln y = -3213x + 2.998$ and $\ln y = -3502x + 4.747$, respectively) and without CTA³ (solid line, $\ln y = -3012x + 4.086$).

References

1. A. R. Maniego, A. T. Sutton, M. Gaborieau and P. Castignolles, *Macromolecules*, 2017, **50**, 9032–9041.
2. A. R. Maniego, D. Ang, Y. Guillaneuf, C. Lefay, D. Gigmès, J. R. Aldrich-Wright, M. Gaborieau and P. Castignolles, *Anal. Bioanal. Chem.*, 2013, **405**, 9009-9020.
3. N. F. G. Wittenberg, C. Preusser, H. Kattner, M. Stach, I. Lacík, R. A. Hutchinson and M. Buback, *Macromol. React. Eng.*, 2015, **10**, 95-107.
4. R. J. Minari, G. Caceres, P. Mandelli, M. M. Yossen, M. Gonzalez-Sierra, J. R. Vega and L. M. Gugliotta, *Macromol. React. Eng.*, 2011, **5**, 223-231.
5. H. Torii, K. Fujimoto and H. Kawaguchi, *J. Polym. Sci. Pol. Chem.*, 1996, **34**, 1237-1243.
6. N. M. Ahmad, B. Charleux, C. Farcet, C. J. Ferguson, S. G. Gaynor, B. S. Hawkett, F. Heatley, B. Klumperman, D. Konkolewicz, P. A. Lovell, K. Matyjaszewski and R. Venkatesh, *Macromol. Rapid Commun.*, 2009, **30**, 2002-2021.
7. A. N. Nikitin, R. A. Hutchinson, G. A. Kalfas, J. R. Richards and C. Bruni, *Macromol. Theory Simul.*, 2009, **18**, 247-258.
8. J.-B. Lena, A. K. Goroncy, J. J. Thevarajah, A. R. Maniego, G. T. Russell, P. Castignolles and M. Gaborieau, *Polymer*, 2017, **114**, 209-220.